Studies on Responses of Tobacco Cells to Boron Deprivation

Taichi Koshiba

2010

Contents

Abbreviations

B	Boron
Ca^{2+}	calcium ion
DW	dry weight
EDTA	ethylenediamine tetraacetic acid
EST	expression Sequence Tag
FW	fresh weight
H_2O_2	hydrogen peroxide
PCD	programmed cell death
RG-II	rhamnogalacturonan II
ROS	reactive oxygen species
RT-PCR	reverse transcription-polymerase chain reaction
Tris	tris(hydroxymethyl) aminomethane

Introduction

Boron (B) is an essential micronutrient for plants. The requirement for B in plant was first demonstrated in broad bean (*Phaseolus vulgaris*) by Warington (1923). Although at that time the requirement for B was not defined in graminaceous monocots, Sommer and Lipman (1926) later demonstrated that Barley (*Hordeum vulgare*) also requires B using repurified reagents and redistilled water. From these and many other studies, B is now recognized as an essential micronutrient for vascular plants in general. Recently, B was shown to stimulate growth of yeast (Bennett et al. 1999) and to be essential for zebrafish (*Danio rerio*) (Eckhert and Rowe 1999; Rowe and Eckhert 1999) and possibly for trout (*Oncorhynchus mykiss*) (Eckhert 1998; Rowe et al. 1998), frogs (*Xenopus laevis*) (Fort et al. 1998), and mouse (*Mus musculus*) (Lanoue et al. 2000). There is also a preliminary evidence suggesting that B is essential, or at least beneficial, for human (Nielsen 2000).

Boron is a member of metalloids and has intermediate properties between metals and non-metals (Marschner 1995). B is widely distributed in both lithosphere and hydrosphere, with concentration ranging from 5~10 mg kg^{-1} in rocks (Shorrocks 1997), 3~30 μg kg^{-1} in rivers (Power and Woods 1997) and ~4.5 mg kg^{-1} in ocean (Lemarchand et al. 2000). Boric acid is a very weak acid with a p*K*a of 9.24. Under the common soil pH values (pH 5.5~7.5), more than 98% of B exists as undissociated boric acid [$B(OH)_3$] and less than 2% as $B(OH)_4^-$ (Woods 1996, Fig. 1). Boric acid, as a borate, forms esters and complexes with a wide variety of mono, di- and poly-hydroxy compounds (Woods 1996). These borate esters form and dissociate spontaneously in dynamic pH-dependent equilibrium and with rapid kinetics (Friedman et al. 1974).

Over the preceding 90 years, much physiological impairments as a result of B deficiency have been reported and it has been postulated that B may be involved in a large number of metabolic pathways. The symptoms of B deficiency include rapid cessation of root elongation, inhibited growth of young leaves and reduced fertility (Blevins and Lukaszewski 1998;

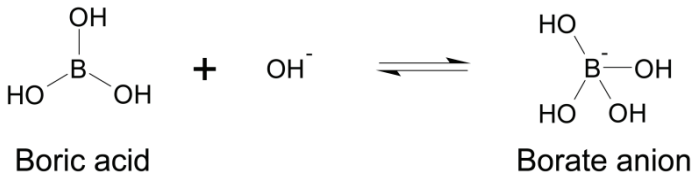

Fig. 1 Interconversion of boric acid and borate anion.

Goldbach and Wimmer 2007). At the cellular level, B deficiency harms numerous physiological processes, including sugar transport, cell wall synthesis, lignification, cell wall structure, carbohydrate metabolism, RNA metabolism, respiration, indoleacetic acid metabolism (Parr and Loughman 1983), cytoskeletal proteins (Yu et al. 2001, 2003), phenolics and polyamines metabolism (Camacho-Cristóbal et al. 2002, 2004, 2005) and membrane potential, plasmalemma-bound enzymes and ion fluxes across membranes (Blaser-Grill et al. 1989; Goldbach et al. 2001), nitrogen metabolism (Camacho-Cristóbal and González-Fontes 1999, 2007), and eventually brings about cell death (Matoh et al. 1992).

There are increasing evidences that B is required for the maintenance of the structure and function of membrane (Cakmak and Römheld 1997; Goldbach et al. 2001; Brown et al. 2002). For example, B deficiency altered the membrane potential and reduced the activity of proton-pumping ATPase in *Helianthus annuus* (Ferrol and Donaire 1992) and *Daucus carota* (Blaser-Grill et al. 1989) roots. It has been also reported that B deficiency alters plasma membrane permeability for ions and other solutes (Cakmak et al. 1995; Wang et al. 1999). However, it is highly unlikely that B works directly in such a diverse physiological process, it remains possible that these metabolic disorders are secondary effects. These reports imply that B would have a certain fundamental role.

A role for B in the cell wall of plants has long been predicted on the basis of several historical observations and broad interpretations of anatomical observations under B deficiency (Loomis and Durst 1992; Brown et al. 2002). Boron is essential for organisms with carbohydrate-rich cell walls (Lewis 1980; Loomis and Durst 1992), and symptoms of B deficiency include the cessation of growth of apical meristems (both shoots and roots) and the

development of brittleness of leaves which has been ascribed to an inhibition of cell wall synthesis or structural integrity (Loomis and Durst 1992; Goldbach 1997). Boron deficiency also results in the formation of cell walls which are abnormally thick (Spurr 1957; Kouchi and Kumazawa 1976; Matoh et al. 1992; Matoh et al. 2000), structurally deformed (Lee and Aronoff 1966; Hu and Brown 1994) and have a coarser than normal texture (Spurr 1957; Matoh et al. 1992). An accumulation of vesicles at the cell wall/membrane interface is also observed (Spurr 1957; Hirsch and Torrey 1980; Matoh et al. 1992; Matoh et al. 2000) while the physical properties of the cell wall become altered very rapidly under B deficient conditions (Findeklee and Goldbach 1996; Findeklee et al. 1997; Goldbach et al. 2001). Furthermore, a significant but variable portion of B in plants is associated with the cell wall (Hu and Brown 1994; Hu et al. 1996; Kobayashi et al. 1997), and this amount differs among species and is correlated with whole plant B requirements (Matoh et al. 1996). Each of these results suggests that B plays an important role in the cell wall.

In the last decade, much progress has been made in understanding the physiological function of B in plants. The protoplasts of tobacco BY-2 cells (*Nicotiana tabacum*) contain as much as 1.6% of cellular B (Matoh et al. 1992), suggesting that essentially all the B in tobacco cells is localized in cell wall. In 1993, Matoh et al. isolated a B-polysaccharide complex from radish roots (Matoh et al. 1993). Kobayashi et al. (1996) found that the B in cell wall occurs as a complex with two rhamnogalacturonan II (RG-II) regions of pectic polysaccharides (Fig. 2). In tobacco cells, at least 70% of the cellular B could be recovered as the B-RG-II complex (the cell wall contained 90% of cellular B and 80% of the cell wall B could be recovered as the complex), suggesting that B fulfills its physiological function via forming this complex. Similar B-RG-II complexes were subsequently purified from bamboo (Kaneko et al. 1997), red wine (Pellerin et al. 1996) and sugar beet pulp (Ishii and Matsunaga 1996). Matoh et al. (1996) demonstrated the occurrence of a B complex with high molecular weight fragments of the cell wall of 24 plant species and suggested that RG-II is the exclusive binding site for B. The complex has been shown to contribute significantly to the control of cell wall porosity (Fleischer et al. 1999) and tensile strength (Ryden et al. 2003). Studies using plants with a mutant RG-II structure showed that the complex is necessary for normal plant growth (O'Neill et al. 2001; Iwai et al. 2002; Ahn

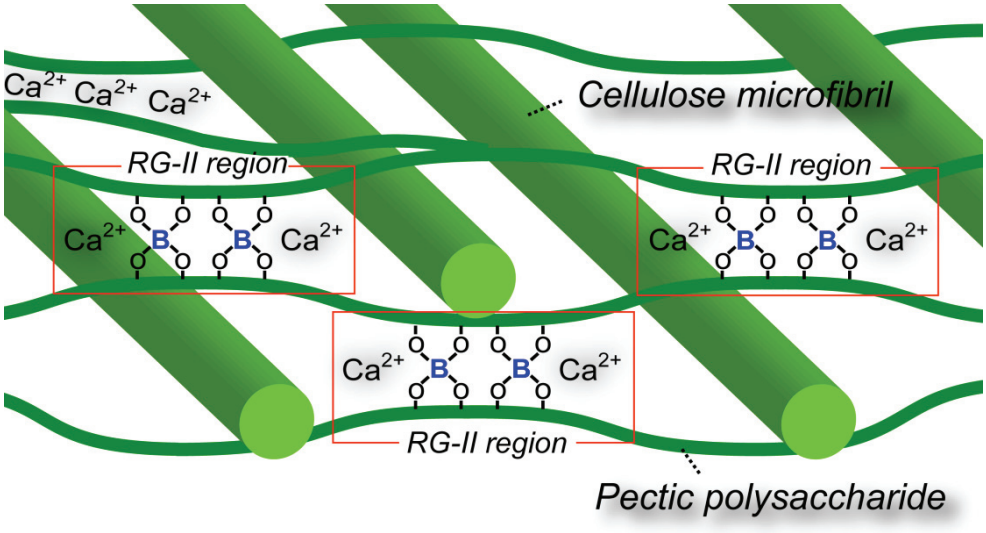

Fig. 2 A schematic diagram of cell wall network.

et al. 2006). These findings together demonstrate that B is essential for cell wall structure and function (O'Neill et al. 2004).

From these studies it is implicated that the primary effect of B shortage is a disturbed structural organization of cell walls. Furthermore, >98% of B localized in cell wall and no molecule other than RG-II has been found to form stable complex with B under physiologically relevant conditions support this suggestion. As Kobayashi et al. (1999) reported that B-RG-II complex stabilized by Ca^{2+} rather stable and does not compose even when B is removed from the surrounding medium, it is conceivable that the events induced by B deficiency are the cause of failure to cross-link newly secreted monomeric RG-II. However, it remains unclear how and why B deficiency, and probably the resulting aberrant cell wall structure, leads to such a variety of metabolic disorders and cell death. Elucidating this process is important for a better understanding of the function of B, and for the development of methods to prevent crop loss due to B deficiency.

Most previous studies on B deficiency have been carried out using intact plants. However, the interpretation of experimental results is complicated because intact plant tissues consist of

various types of differentiated cells which probably differ in their requirements for B. In addition, since only a proportion of the cells in a tissue are in direct contact with the external solution, most cells might remain unaffected when B is withdrawn from the medium. These experimental problems might be circumvented by the use of suspension-cultured cells, as they are uniform and their surrounding media are easy to control. Cultured tobacco BY-2 cells are especially suitable because they do not aggregate significantly, and essentially all the cells are in direct contact with the external medium. Moreover, their death process has been characterized in detail in recent studies (de Pinto et al. 2002; Vacca et al. 2004; de Pinto et al. 2006).

In this study, I took advantage of suspension-cultured tobacco BY-2 cells for the study of B nutrition, and investigated their responses to B deprivation in detail. I revealed that oxidative damage is the direct cause of cell death induced by B deprivation, and the mode of cell death is not a typical programmed cell death but necrosis (Chapter 1). I found that the cells deprived of B changed their gene expression as an adaptive response to oxidative stress (Chapter 2). Finally, I found that the increased expression of B-deprivation responsive gene is dependent on Ca^{2+} influx, and that Ca^{2+} influx is possibly mediated by stretch-activated Ca^{2+} channels (Chapter 3). These results suggest that, in tobacco cells, failure to form B-RG-II complex causes oxidative damage which eventually leads to necrosis.

Chapter 1

Mechanism of Cell Death Induced by Boron Deprivation

1.1 Introduction

In cultured tobacco cells, more than 98% of B is localized in cell wall (Matoh et al. 1992), and the B as a borate cross-link two RG-II regions of pectic polysaccharides in the cell wall (Kobayashi et al. 1996). Studies using plants with a mutant RG-II structure showed that the B-RG-II complex is necessary for normal plant growth (O'Neill et al. 2001; Iwai et al. 2002; Ahn et al. 2006), and now B has been established as essential for cell wall structure and function (O'Neill et al. 2004). Previous reports show that B shortage affects the properties of cell wall. Goldbach's group reported that the physical properties of squash root cell walls change within minutes after B deprivation (Findeklee et al. 1997; Goldbach et al. 2001). Matoh et al. (2000) reported that low B-acclimated tobacco BY-2 cells have swollen cell wall, and two-thirds of the RG-II in these cells occurs in a monomeric form, whereas all the RG-II occurs as a dimer cross-linked with B in the parent cells. These findings imply that the primary effect of B shortage is to disturb the structural organization of cell wall. However, it remains unclear why B deficiency, and probably the resulting aberrant cell wall structure, leads to various metabolic disorders and cell death. To understand this mechanism, in this chapter I characterize the B deprivation-induced cell death of tobacco cells.

1.2 Materials and methods

1.2.1 Cell culture and treatments

Suspension–cultured tobacco cells (*Nicotiana tabacum* L. cv. Bright Yellow-2) were cultured at 25°C as described previously (Nagata et al. 1981) and maintained by transferring a 5 ml aliquot of a 7-day-old culture into 75 ml of fresh medium.

The B-free medium was prepared as described previously (Matoh et al. 1992).

Three-day-old cells (150 ml cell suspension) were collected on a 60-μm nylon mesh filter by gravity flow and were divided into two aliquots. Each aliquot was suspended in 400 ml of B-free or control (1 mg B liter^{-1}, Nagata et al. 1981) culture medium for 1 min and was filtered. After repeating the process three times, cells were transferred to a plastic (polymethylpentene) flask containing 75 ml of the corresponding B-free or control medium.

For butylated hydoxyanisole (BHA) or α-tocopherol treatment, cells were pre-cultured in the control medium supplemented with 0.1 mM of either BHA (Sigma-Aldrich, St Louis, MO, USA) or α-tocopherol (Nacalai Tesque, Kyoto, Japan) for 1 h, then washed with and transferred to the medium supplemented with 0.1 mM of BHA or α-tocopherol, as above. BHA and α-tocopherol were diluted from a 100 mM stock solution in methanol or ethanol, respectively. For cycloheximide (CHX) treatment, cells were pre-cultured in control medium supplemented with 0.35 μM CHX (Nacalai Tesque) for 1 h, then washed with and transferred to medium supplemented with 0.35 μM CHX. CHX was diluted from a 0.35 mM stock solution in methanol.

1.2.2 Determination of cell viability

To the cell suspension was added 7.5 μg ml^{-1} fluorescein diacetate (FDA; Sigma-Aldrich) and 22.5 μg ml^{-1} propidium iodide (PI; Wako Pure Chemicals, Osaka, Japan) and they were incubated for 10 min at room temperature. Samples were observed under a fluorescence microscope (BX-51, Olympus, Tokyo, Japan) with a 460-495 nm excitation filter and a 510 nm barrier filter, to distinguish the dead (red) and live (green) cells. Cell viability was calculated from the counts of four randomly selected fields, in which at least 200 cells were present. Cell numbers were counted with a 0.2 mm depth hematocytometer.

1.2.3 Detection of ROS

The assay was performed according to Yamamoto et al. (2002) with some modifications. Dihydroethidium (DHE) was added to the cell suspension at a final concentration of 10 μM. After incubation at 25°C for 30 min in the dark, cells were observed for ethidium fluorescence under a fluorescent microscope (Olympus BX-51), with a 510-530 nm excitation filter and a 575 nm barrier filter.

1.2.4 DNA fragmentation analysis

Genomic DNA was prepared by the cetyltrimethylammonium bromide method (Murray and Thompson 1980). Samples were treated with 100 μg ml^{-1} DNase-free RNase (Nacalai Tesque) for 1 h at 37°C and electrophoresed on a 1.8% (w/v) agarose gel followed by visualization with ethidium bromide. As a positive control for DNA laddering, genomic DNA prepared from heat-shocked cells was run alongside (Vacca et al. 2004).

1.2.5 Determination of lipid peroxides

Lipid peroxides were quantified by the thiobarbituric acid reactive substances (TBARS) method as malondialdehyde equivalents, with 1,1,3,3,-tetramethoxypropane as the standard (Yagi 1984; Jagendorf and Takabe 2001). Tobacco cells were harvested by vacuum filtration and were ground in liquid nitrogen to a fine powder with a mortar and pestle. A 50 mg aliquot of the powder was mixed with 1.0 ml of ice-cold 10% (w/v) trichloroacetic acid, left on ice for 1 h and centrifuged at 12,000×g for 20 min at 4°C. A 0.4 ml aliquot of the supernatant was transferred to a glass test tube, mixed with 1.8 ml of 10% (w/v) trichloroacetic acid, 0.01 ml of 2% (w/v) butylated hydroxytoluene in ethanol, and 0.2 ml of 3% (w/v) thiobarbituric acid, and then boiled for 60 min. After cooling on ice, the mixture was centrifuged at 700×g for 10 min and the fluorescence of the supernatant was measured at 515 nm excitation and 553 nm emission wavelengths.

1.2.6 Determination of ascorbate and glutathione

Cells were harvested by vacuum filtration and were ground in liquid nitrogen to a fine powder with a mortar and pestle. To determine reduced ascorbic acid (ASC), 100 mg of the pulverized cells were mixed with 0.4 ml of ice-cold 5% (w/v) metaphosphoric acid and centrifuged at 12,000×g for 10 min at 4°C. The supernatant was filtered through a 0.2 μm filter (GL Chromatodisk 4A, GL Sciences, Tokyo, Japan) and 20 μl aliquots were separated by HPLC (LC-10A HPLC system, Shimadzu, Kyoto, Japan). The column (Unison UK-C18, 4.6×100 mm, Imtakt, Kyoto, Japan) was equilibrated and eluted with 20 mM potassium phosphate (pH 7.0) containing 10 mM tetrabutylammonium bromide at a flow rate of 1 ml min^{-1}. Ascorbate was detected at 265 nm. To determine total ascorbate [ASC + dehydroascorbate (DHA)], HPLC

samples were added with 5 mM dithiothreitol and were incubated for 30 min in the dark at 25°C before analyses.

Glutathione (GSH) was quantified as described by Klapheck et al. (1994) with some modifications. A 50 mg aliquot of the pulverized cells was mixed with 0.8 ml of ice-cold 0.1 M HCl and centrifuged at 12,000×g for 10 min at 4°C. The supernatant was transferred to a new centrifuge tube, and added with trifluoroacetic acid (TFA) to a final concentration of 5% (v/v). The precipitate formed was removed by centrifugation at 12,000×g for 10 min at 4°C, and 20 µl aliquots were separated by HPLC (LC-10A HPLC system). The column (Cosmosil $5C_{18}$-PAQ, 5 µm corn size, 4.6×150 mm, Nacalai Tesque) was equilibrated and eluted with 0.05% (v/v) TFA at a flow rate of 0.8 ml min^{-1}. To the column eluent, 75 µM 5,5'-dithiobis(2-nitrobenzoic acid) in 50 mM potassium phosphate (pH 8.0) was added at 0.8 ml min^{-1}, and the mixture was allowed to pass through a reaction loop of 0.5 mm×3 m at 30°C. The derivatized GSH was detected at 410 nm.

1.2.7 Antioxidant enzyme assays

Enzymes were extracted at 0-4°C from 100 mg of pulverized cells with 0.4 ml of one of the following media: superoxide dismutase (SOD; EC 1.15.1.1), 100 mM potassium phosphate (pH 7.8), 0.1 mM EDTA and 0.1% (v/v) Triton X-100; catalase (CAT; EC 1.11.1.6), 100 mM potassium phosphate (pH 7.0) and 0.1 mM EDTA; ascorbate peroxidase (APX; EC 1.11.1.11), 50 mM potassium phosphate (pH 7.8) and 1 mM ASC. The extracts were centrifuged at 12,000×g for 10 min at 4°C, and the supernatants were used for the assays.

SOD activity was determined using a SOD Assay Kit-WST (Dojindo Molecular Technologies, Kumamoto, Japan) according to the manufacturer's instructions. One unit of SOD activity was defined as the amount required to inhibit the reduction of tetrazolium by 50%. CAT activity was determined by following the consumption of H_2O_2 (extinction coefficient 39.4 mM^{-1} cm^{-1}) at 240 nm for 30 s (Aebi 1984) in a 3 ml reaction mixture containing 50 mM potassium phosphate (pH 7.0), 10 mM H_2O_2 and 200 µl of the extract. APX activity was determined by following the consumption of ASC (extinction coefficient 2.8 mM^{-1} cm^{-1}) at 290 nm for 30 s, in a 1 ml reaction mixture containing 50 mM potassium phosphate (pH 7.0), 0.1 mM EDTA, 0.5 mM ASC, 0.1 mM H_2O_2 and 4 µl of the extracts (Asada 1984). Soluble protein contents were determined as described previously (Bradford, 1976), with bovine serum albumin

as the standard.

1.2.8 Semi-quantitative RT-PCR analysis

Total RNA was isolated by phenol:chloroform extraction and LiCl precipitation (Shirzadegan et al. 1991), and genomic DNA contamination was eliminated by treatment with RNase-free DNase (TAKARA BIO INC., Shiga, Japan). First-strand cDNA was synthesized using ReverTra Ace DNA polymerase (Toyobo, Osaka, Japan) in a 25 µl reaction mixture, containing 1 µg of total RNA and 2.5 pmol $(dT)_{18}$ primer. The reactions were performed at 42°C for 60 min followed by 95°C for 5 min. The reaction mixture was diluted 4-fold with 10 mM Tris-HCl (pH 8.0) and 1 mM EDTA, and 1 µl aliquots were used for PCR with rTaq DNA polymerase (Toyobo) in a final volume of 25 µl. A 699 bp cDNA fragment of cAPX (accession No. D85912) was amplified using the primers 5'-CACTGTAAGCGAGGAGTACC-3' and 5'-TGAGCCTCAGCATAGTCAGC-3' (Vacca et al. 2004). A 493 bp cDNA fragment of actin (accession No. AB158612) was amplified using the primers 5'-AAGGTTACGCCCTTCCTCAT-3' and 5'-GCCACCACCTTGATCTTCAT-3', to calibrate the quantities of cDNA templates. PCR was performed with arbitrary cycles of 94°C for 30 s, 55°C for 30 s and 72°C for 30 s. The PCR products were analyzed on a 1% (w/v) agarose gel and were visualized with ethidium bromide.

1.3 Results

Boron deprivation-induced oxidative damage to tobacco cells

First I examined the effects of B deprivation on the viability of tobacco BY-2 cells. Three-day-old cultures, which were in the log phase of growth, were used in this study. Cells were washed with medium with or without B, and then cultured in the same medium (hereafter referred to as +B or –B treatment, respectively). Cell viability was analyzed by FDA/PI staining, and a representative result is shown in Fig. 1.1a. With +B treatment, dead cells comprised <3% of the total cells throughout the experimental period (Fig. 1.1a). In contrast, with –B treatment, cell death was detectable as early as 12 h after treatment, and the viability decreased to 30% by 48 h (Fig. 1.1a). When total cells, dead or alive, were counted 24 h after treatment, the –B culture contained 60-70% as many cells as the +B culture did (data not presented). Since the

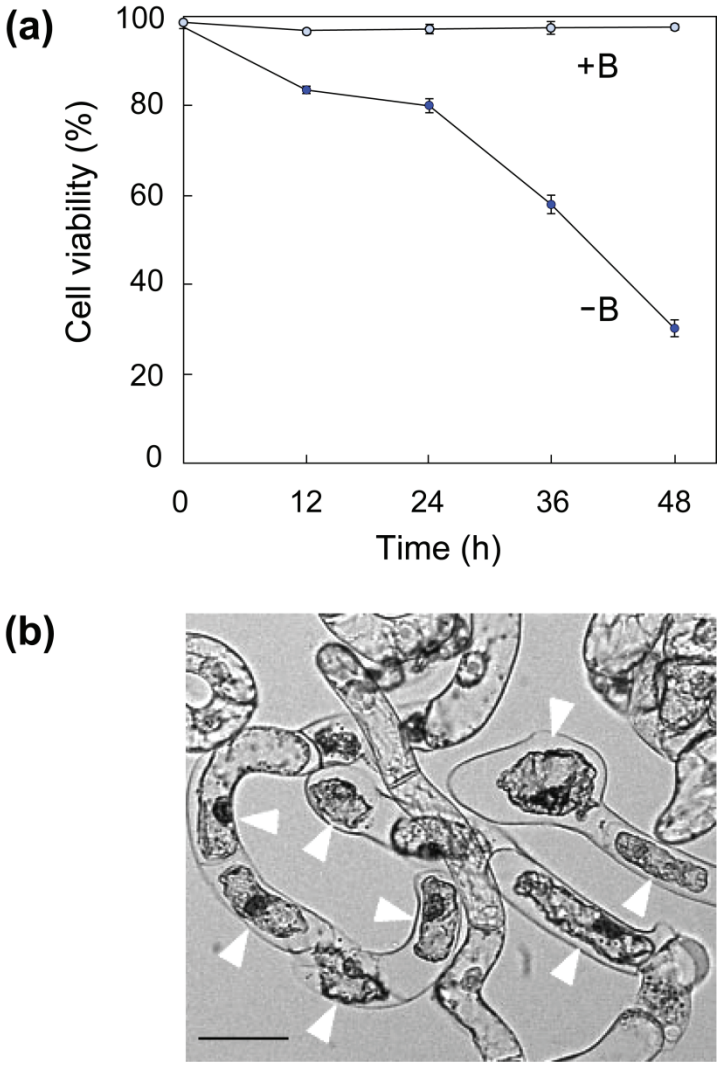

Fig. 1.1 Cell death induced by B deprivation. **(a)** The time-dependent change of cell viability. Cells were washed with and cultured in control (+B) or B-free (–B) media and were examined for viability with FDA/PI staining. Values represent the percentage of FDA-stained live cells, which is an average of the results obtained from four randomly selected fields. **(b)** Morphology of dead cells in –B culture. Cells were observed under bright–field microscopy 48 h after treatment. Arrowheads indicate dead cells. Bar = 50 μm.

proportion of live proliferating cells in the –B culture had already decreased to approximately 80% at 12 h (Fig. 1.1a), and since the doubling time of tobacco BY-2 cells is approximately 12 h (Nagata et al. 1992), the –B culture would be predicted to contain around 70% as many cells as the +B culture at 24 h, if cell division is not affected by the treatment. The predicted cell number

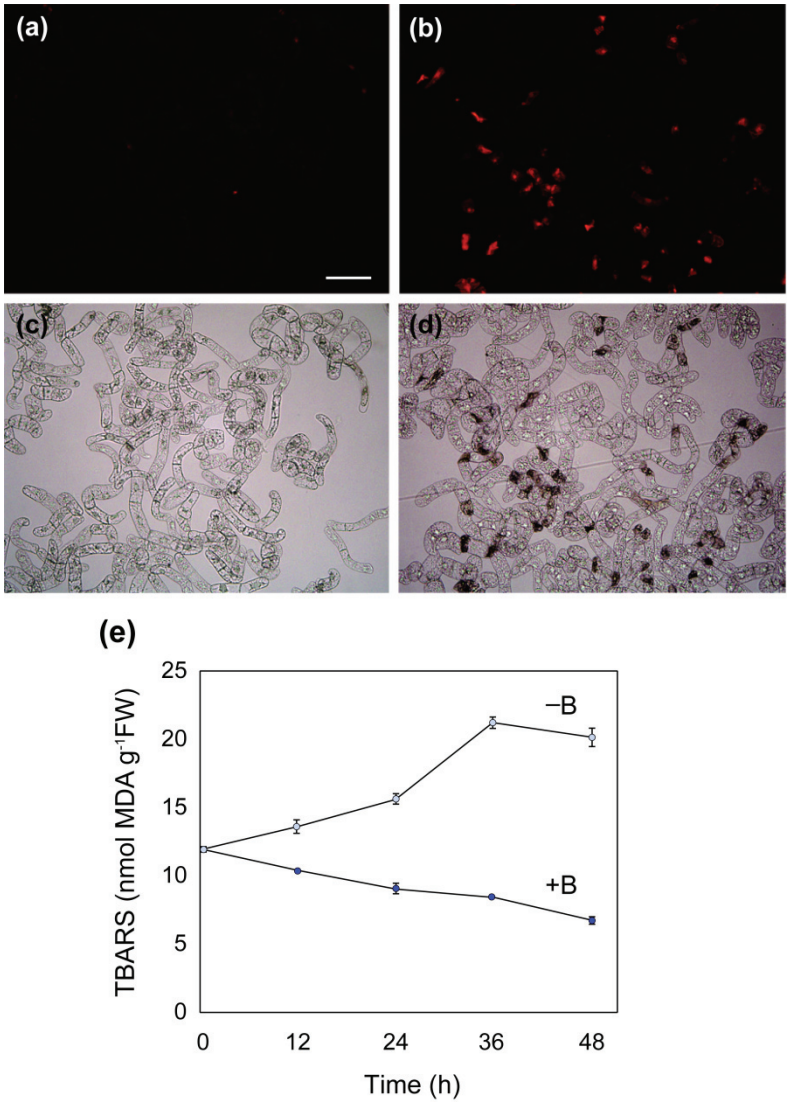

Fig. 1.2 Oxidative stress induced by B deprivation. **(a-d)** Accumulation of ROS. At 12 h after treatment, +B **(a, c)** or –B **(b, d)** cells were stained with DHE and observed under fluorescence **(a, b)** or bright-field **(c, d)** microscopy. Bar = 100 µm. **(e)** Accumulation of lipid peroxides. Lipid peroxides were quantified by the TBARS method and expressed as nmol malondialdehyde (MDA) per gram fresh weight. Each value is the mean of two replicates and the error bar represents the difference between the replicates.

is consistent with the observed results, suggesting that cell division was not significantly impaired upon B deprivation. Microscopic examination of dead cells in the –B culture revealed a characteristic morphology with a shrunken cytoplasm (Fig. 1.1b).

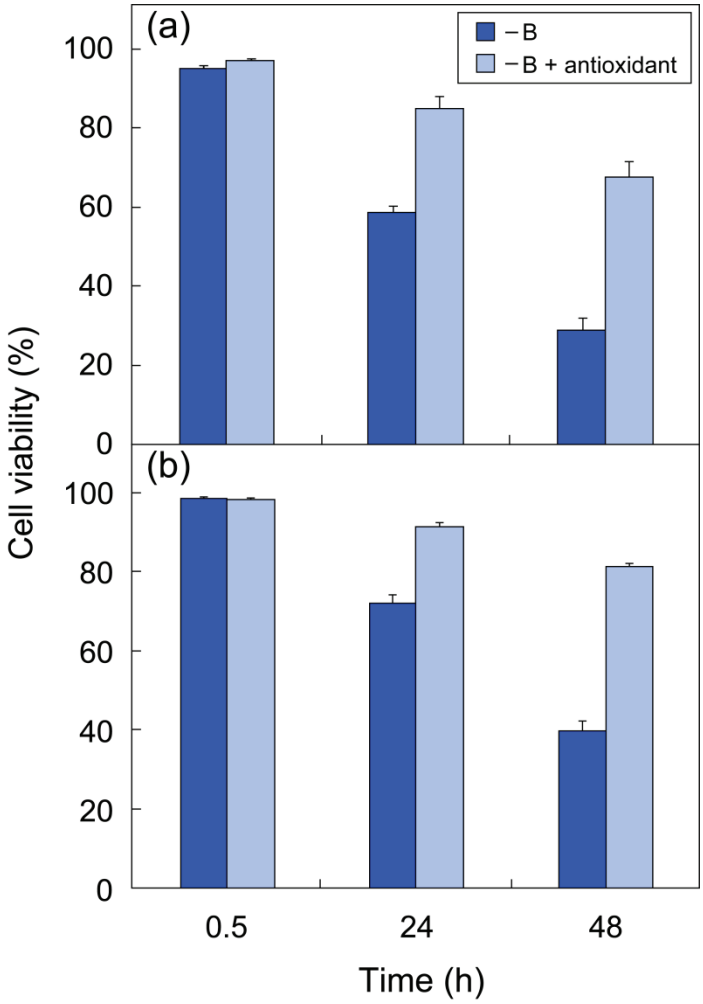

Fig. 1.3 Effect of antioxidant on cell death induced by B deprivation. After pre-culture for 1 h in a standard growth medium supplemented with 0.1 mM of either BHA **(a)** or α-tocopherol **(b)**, cells were washed with and transferred to a B-free medium supplemented with the same 0.1 mM antioxidant. Cells treated in the same way but without antioxidant were prepared as a control. Each bar shows the mean of results from four randomly selected fields ± SD.

Kobayashi et al. (2004) previously showed that the genes for antioxidant enzymes are up-regulated in low B-acclimated cells, which suggests that oxidative damage is involved in low B stress. To test this hypothesis, I examined the accumulation of reactive oxygen species (ROS) in –B cells, using DHE as a probe. In the presence of ROS, DHE is oxidized to ethidium that intercalates with DNA to emit red fluorescence. As shown in Fig. 1.2a-d, the ethidium-derived fluorescence was detectable at 12 h in –B cells, but not in +B cells. This result indicates that

ROS accumulated in –B cells. I then analyzed lipid peroxidation in these cells as a measure of oxidative damage, using the TBARS assay. TBARS are the product of lipid peroxidation, and high levels of these substances correlate with high levels of oxidative damage to membranes (Heath and Packer 1968). As shown in Fig. 1.2e, more TBARS accumulated in –B cells than in +B cells as early as 12 h, and the levels in –B cells increased even further over time. If oxidative damage plays a critical role in cell death induced by B deprivation, then this cell death would be expected to be suppressed by the addition of antioxidants. I therefore examined the effect of BHA, a lipophilic antioxidant that reportedly prevents antimycin A- or aluminum stress-induced ROS accumulation (Maxwell et al. 1999, Yamamoto et al. 2002), upon B deprivation-induced cell death. Supplementing the medium with BHA at 0.1 mM did not affect the viability of +B cells (data not shown). On the other hand, it significantly improved the viability of –B cells (Fig. 1.3a). α-Tocopherol, another lipophilic antioxidant, also suppressed the death of –B cells (Fig. 1.3b). Although the cells in Fig. 1.3b were fed with α-tocopherol prior to the treatment, adding α-tocopherol after B removal was also effective (data not shown). These results were not attributable to contaminating B in the reagents; possible B contamination from BHA or α-tocopherol was estimated to be <0.03 μg B liter^{-1}, which is far lower than the amount remaining in the B-depleted medium (typically 2-5 μg B liter^{-1}).

Effects of B resupply

When B (1 mg liter^{-1} as boric acid) was resupplied to the cells that had been deprived of B for 24 h, the cell viability at 48 h (24 h after resupply) was as high as 68%, significantly higher than for cells remaining in –B medium for the same period (30%; Fig. 1.1a). I next counted the number of dead cells to investigate the effect of B resupply on cell viability. For this analysis, duplicate cultures were deprived of B, and then supplemented after 18 h with either boric acid at 1 mg B liter^{-1} (‘resupplied culture’) or water (‘–B culture’). Cells washed with and cultured in control medium were also prepared as a control (‘+B culture’). Cultures that had been deprived of B for 18 h (–B and resupplied cultures) contained significantly more dead cells than the control (+B culture) (Fig. 1.4a). However, during the subsequent 30 h, while the number of dead cells increased further in the –B culture, it did not increase further in the resupplied culture (Fig. 1.4a).

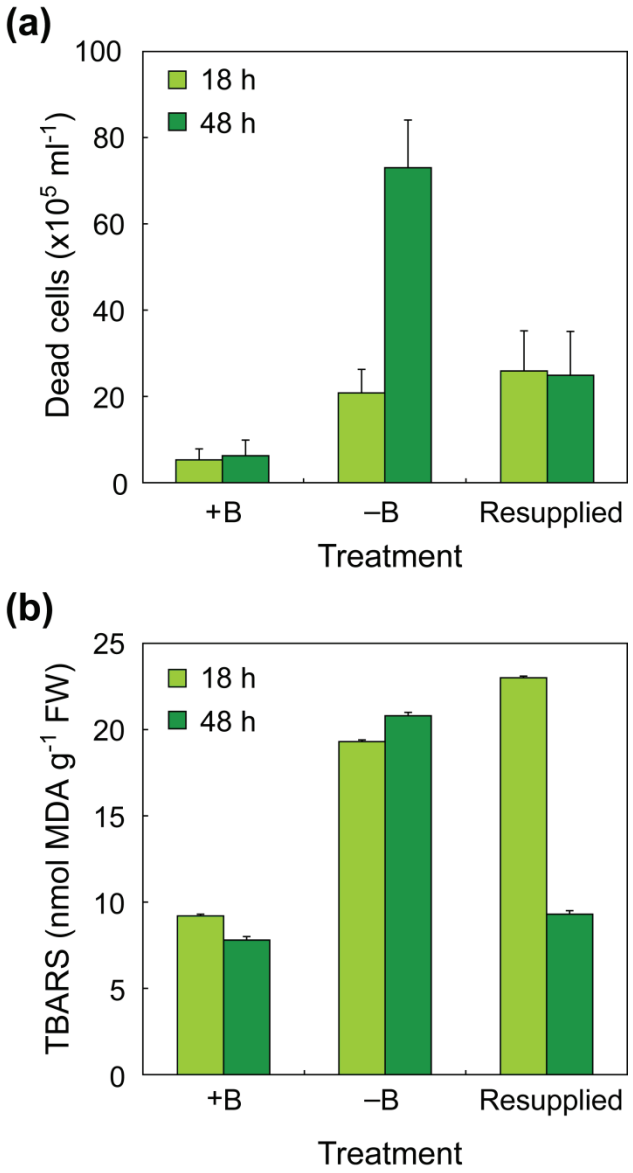

Fig. 1.4 Effects of B resupply on cell death and the accumulation of lipid peroxides. **(a)** Number of dead cells. Duplicate cultures were deprived of B, and then supplemented after 18 h with either boric acid at 1 mg B liter^{-1} ('resupplied culture') or water ('–B culture'). Cells washed with and cultured in control medium were also prepared as a control ('+B culture'). Aliquots of the cell suspensions were withdrawn and dead cells were counted after FDA/PI staining. Each value is an average of the results of six independent counts. **(b)** Lipid peroxide contents. Cells were treated as in **(a)** and their lipid peroxides were quantified as in Fig. 2e. Each value is the mean of two replicates, and the error bar represents the difference between replicates.

Resupplying B at 24 h gave essentially the same results; the dead cell number was 33 ± 5 × 10^5 ml^{-1} at the time of resupply (24 h), and 32 ± 7 × 10^5 ml^{-1} at 24 h after resupply (48 h). These results indicate that the B resupply immediately suppressed further cell death and allowed the surviving cells to resume proliferation.

B resupply also suppressed lipid peroxidation. At 18 h after B deprivation, –B cultures contained twice as much TBARS as +B cultures (Fig. 1.4b). However, by 48 h, the TBARS in resupplied cultures decreased to the same level as that in the +B cultures, whereas it increased even further in the –B cultures (Fig. 1.4b). Taken together, these results indicate that the B deprivation-induced oxidative stress was removed immediately upon B resupply.

Antioxidants and antioxidant enzyme activities

I next explored possible changes in cellular antioxidant systems in cells deprived of B. To detect any change that precedes oxidative injury, the analyses were done at 24 h, when >80% of the cells were still alive (Fig. 1.1a). When compared with +B cells, –B cells did not show a marked decrease in the activities of antioxidant enzymes such as SOD, CAT and APX (Fig. 1.5a). I then examined changes in the pools of reduced GSH and total ascorbate (ASC plus DHA). The quantity of both antioxidants showed transient increases during the first 12 h in both +B and –B cells, probably in response to the mechanical stress imposed by the cell washing procedure (Fig. 1.5b). The GSH content of –B cells was not significantly lower than that of +B cells at any of the time points observed (Fig. 1.5b, upper panel). On the other hand, the total ascorbate pool in 12 h –B cells was decreased by 20% with respect to +B cells (Fig. 1.5b, lower panel), although the ASC redox state (reduced ASC/total ASC) was unaffected (0.89 for both +B and –B cells). The change in total ascorbate pool appears rather marginal, but may nevertheless be directly involved in the oxidative damage since resupply of B at 3 h restored the total ascorbate pool at 12 h to the same level as that observed in 12 h +B cells (Fig. 1.5b).

The mode of cell death induced by B deprivation

Dead cells in –B culture exhibited a shrunken cytoplasm (Fig. 1.1b), which is often observed in plant cells undergoing programmed cell death (PCD) (van Doorn and Woltering 2005). This observation prompted me to investigate whether PCD is also involved in the cell death induced by B deprivation. I first examined internucleosomal genomic DNA fragmentation in –B cells,

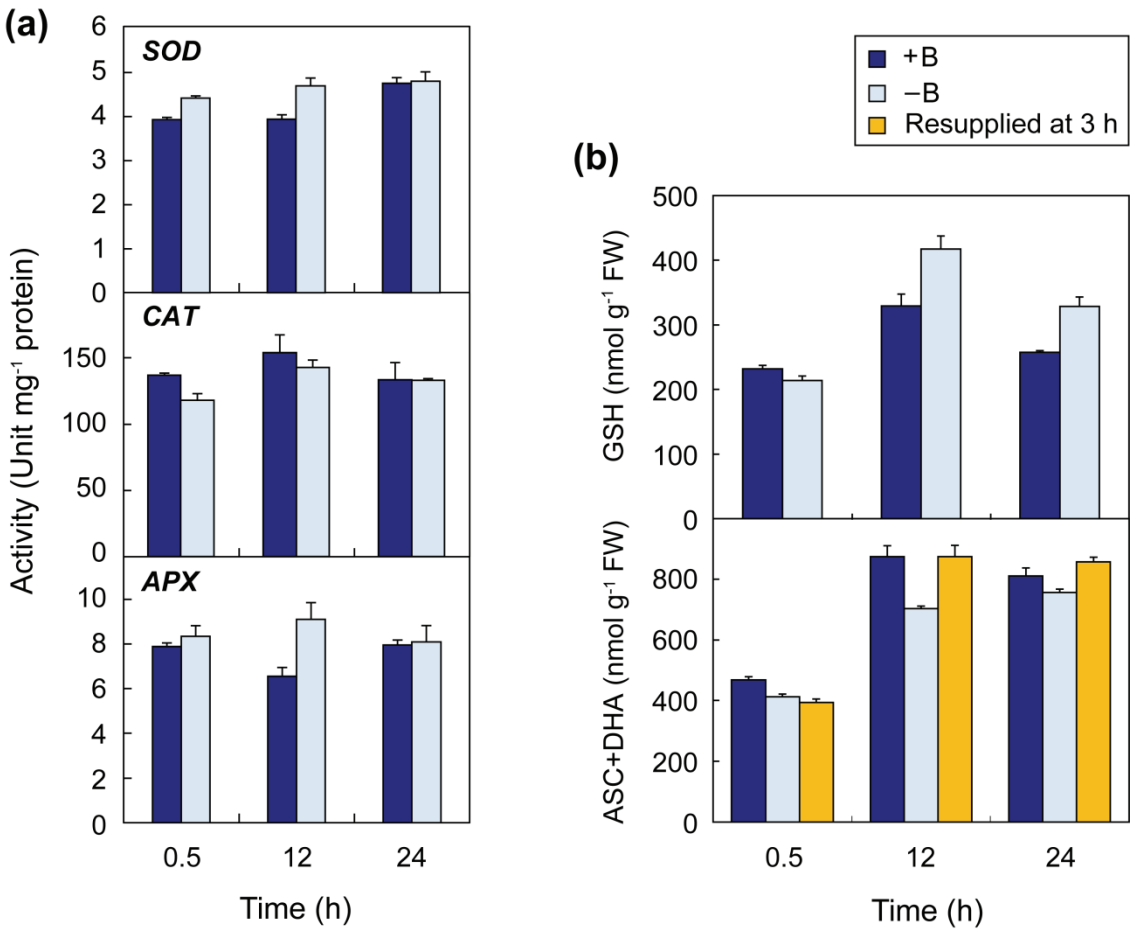

Fig. 1.5 Change in antioxidant capacity. **(a)** Antioxidant enzyme activities. Each value is the mean of three replicates ± SD. **(b)** Changes in contents of reduced GSH (upper panel) and total ascorbate (lower panel). Total ascorbate was also analyzed in the cells resupplied with B at 3 h. Each value is the mean of four (GSH) and three (total ascorbate) replicates ± SD, respectively.

one of the hallmarks of PCD (van Doorn and Woltering 2005). As shown in Fig. 1.6a, clear laddering was observed with DNA extracted from heat-shocked cells, a positive control for PCD (Vacca et al. 2004). On the other hand, smearing rather than laddering was observed with DNAs extracted from –B cells (Fig. 1.6a).

I also examined the effect of CHX on B deprivation–induced cell death. CHX has been reported to suppress PCD by inhibiting the synthesis of proteins that are required to execute the death program (Solomon et al. 1999; Clarke et al. 2000; Vacca et al. 2004; Duval et al. 2005). If PCD is involved, then supplementing the medium with CHX should suppress death induced by

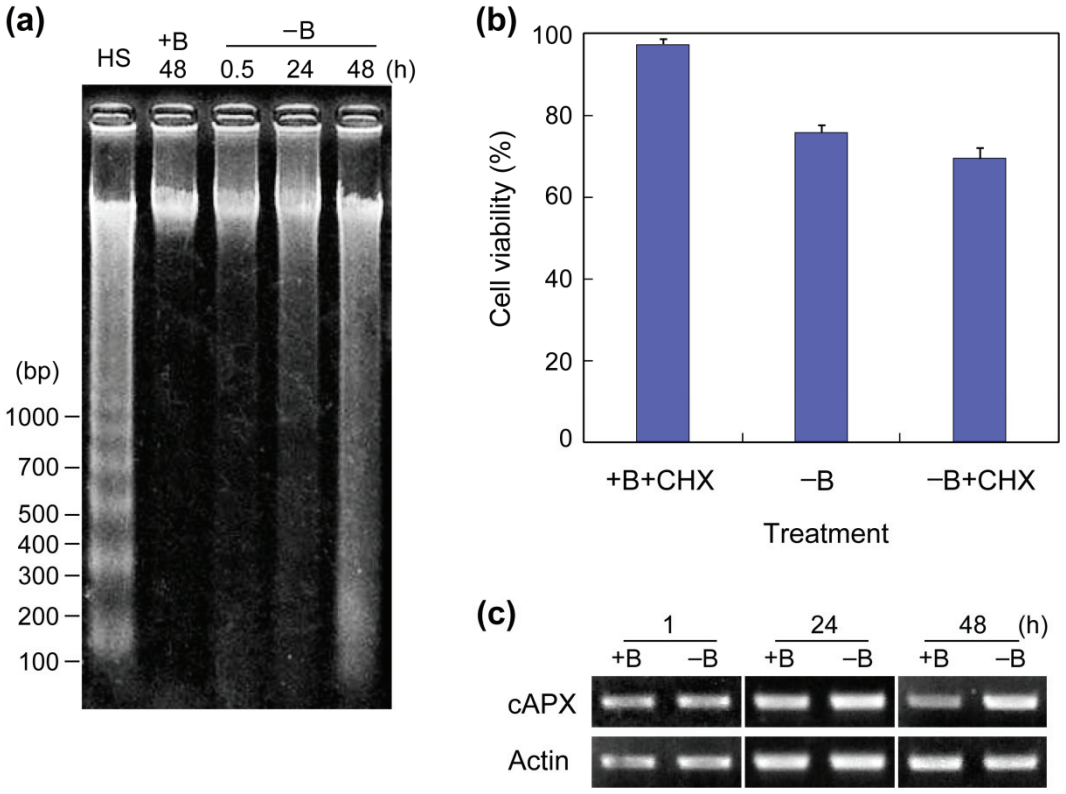

Fig. 1.6 (a) DNA fragmentation analysis. Genomic DNA was extracted from cells at the indicated times after treatment. As a positive control for DNA laddering, DNA extracted from heat-shocked cells was included in the analysis (lane HS, DNA was extracted 72 h after treatment). The figure shows a representative result in which 400 ng of DNA was run in each lane. **(b)** Effect of CHX. Cells were treated as in Fig. 3 except that 0.35 μM CHX was used instead of antioxidants. Each bar shows the mean of results on four randomly selected fields ± SD. **(c)** Gene expression of cAPX. Semi-quantitative RT-PCR for cAPX was performed as described in the text. RT-PCR for the actin gene was also performed to calibrate the quantities of cDNA templates.

B deprivation. As a positive control for the CHX rescue effect, I confirmed that heat shock–induced PCD could be suppressed by 0.35 μM CHX (cell viability at 24 h was 30 ± 7% and 54 ± 3% in the absence or presence of CHX, respectively). However, the viability of –B cells in the presence of CHX (0.35 μM) was 70 ± 3% at 24 h after B deprivation, not significantly different from the viability in the absence of CHX (76 ± 2%), indicating that CHX that heat shock–induced PCD could be suppressed by 0.35 μM CHX (cell viability at 24 h was 30 ± 7% and 54 ± 3% in the absence or presence of CHX, respectively). However, the viability

of –B cells in the presence of CHX (0.35 μM) was 70 ± 3% at 24 h after B deprivation, not significantly different from the viability in the absence of CHX (76 ± 2%), indicating that CHX did not suppress the death induced by B deprivation (Fig. 1.6b).

It has been reported that, in tobacco BY-2 cells, different kinds of cell death (PCD or cell necrosis) have different effects on cellular antioxidant systems (de Pinto et al. 2002; Vacca et al. 2004; de Pinto et al. 2006). One of the most distinctive differences is that the gene expression of cytosolic APX (*cAPX*) is down-regulated during PCD, but not during cell necrosis (de Pinto et al. 2006). I therefore examined *cAPX* expression as another diagnostic feature of PCD, but found the transcript at similar levels in –B cells and +B cells (Fig. 1.6c).

I also examined the morphological differences during –B cells and each cells treated with –Ca, heat shock, 5 mM H_2O_2, 20% ethanol and 0.2 M NaCl (Fig. 1.7). Heat shock and H_2O_2 treatments were used as the PCD control, ethanol and NaCl as the necrosis control. The morphology of –B cells examined under bright-field microscopy was similar to that of heat shock- and NaCl-treated cells (Fig. 1.7 DIC). Under fluorescence microscopy, strong fluorescence were observed in nucleus and probably plasma membrane of –B cells, while in the other cells fluorescence were observed only in nucleus (Fig. 1.7 PI-stain). Taken together, these data suggest that cell death induced by B deprivation is not likely to be a typical PCD.

1.4 Discussion

In this study I have described the physiological responses of suspension–cultured tobacco BY-2 cells to B deprivation, and have shown that ROS and lipid peroxides are accumulated in these cells. These results unequivocally demonstrate that B deprivation causes oxidative damage to the cells as a downstream effect. Previous studies have shown that B deficiency symptoms of *Lemna* are exaggerated under high light conditions (Tanaka 1966), that the cellular antioxidant pool decreases significantly in sunflower or squash under B deficiency (Cakmak et al. 1995; Lukaszewski and Blevins 1996; Cakmak and Römheld 1997) and that oxidative stress-responsive genes are up–regulated in low B-acclimated tobacco cells (Kobayashi et al. 2004). Although these observations are all consistent with the notion that oxidative injuries occur under B deficiency, none of these reports demonstrated that ROS accumulate in the cells. In the present study, I demonstrated the accumulation of ROS and lipid peroxides using DHE staining and TBARS assays. To my knowledge, this is the first direct proof that B-deficient cells

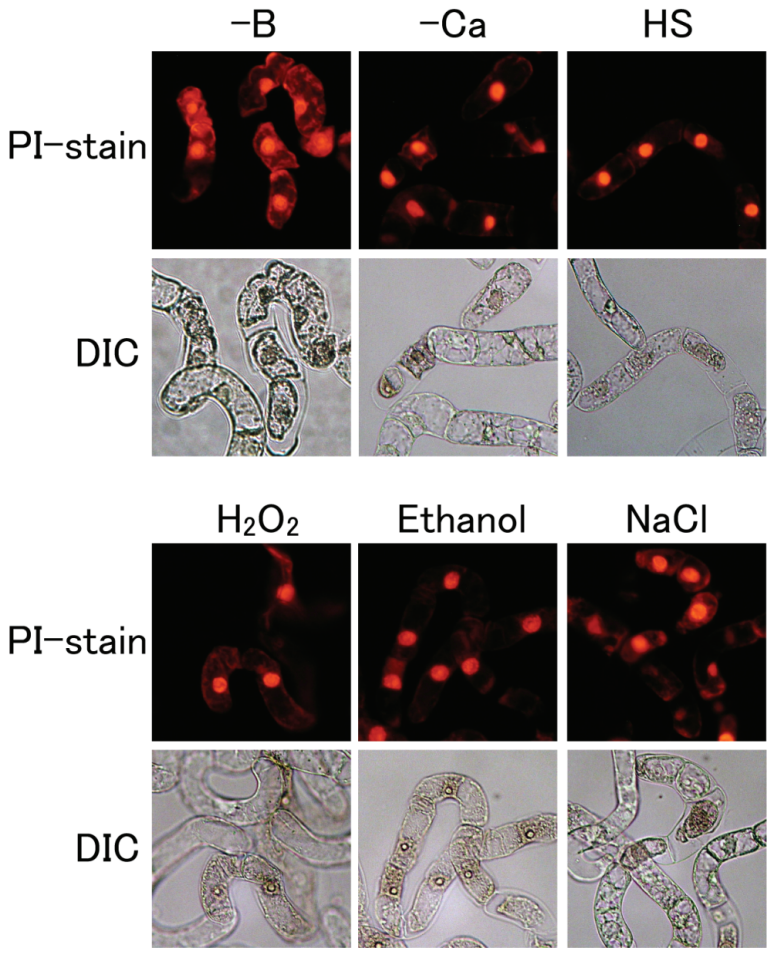

Fig. 1.7 Morphology of cells killed by various treatments. Cells were deprived of B (–B) or Ca (–Ca), heat-shocked for 10 min at 55°C (HS), treated with 5mM H_2O_2 (H_2O_2), 20% ethanol (Ethanol) or 0.2 M NaCl (NaCl), and then cultured for 24 h. Cells were stained with PI and observed under fluorescence **(PI-stain)** or bright–field **(DIC)** microscopy.

suffer from oxidative damage.

Importantly, I furthermore demonstrated that B deprivation-induced cell death was effectively suppressed by lipophilic antioxidants (Fig. 1.3). This result indicates that oxidative damage is crucial and immediately responsible for the death of tobacco cells induced by B deprivation. Obviously, oxidative damage is not unique to B deficiency, but rather represents a consequential effect of the B deficiency stress. Nonetheless, the results are significant in that I have demonstrated that the oxidative damage is the major cause of death under B deficiency,

and therefore plant cells could be less susceptible to B limitation if the oxidative stress can be circumvented. These results also suggest that enhancing the endogenous antioxidant capacity may be one of strategies for engineering B-efficient crops.

It is still debatable whether B plays a direct role(s) in membrane stabilization (Brown et al. 2002). The premise for this hypothesis is that B deprivation makes the plasma membrane depolarized and leaky (Brown et al. 2002). However, given that oxidative damage occurs under B deficiency, the observations of impaired membrane function could be attributed to membrane lipid peroxidation and may not necessarily be the direct effect of B deprivation. In addition, no membrane-associated compound has yet been demonstrated to occur as a complex with B in plant cells. Taken together, I consider that B is unlikely to function primarily as a membrane stabilizer.

Although the dead cells in –B cultures were morphologically similar to those undergoing PCD (Fig. 1.1b, Fig. 1.7 DIC), they did not show other PCD hallmarks such as DNA laddering, decreased *cAPX* expression or protection from death by CHX. Besides –B cells had a characteristic fluorescence in probable plasma membrane. Those fluorescence was not occurred in other treated cells (Fig. 1.7 PI-stain). The immediate rescue effect of B resupply also does not support the involvement of PCD; if the death had been 'programmed' and initiated in –B cells before the morphological changes became visible, then B resupply at 18 h, when a substantial proportion of the cells are already dead (Fig. 1.1a), would not be able to suppress the subsequent cell death. In contrast, B resupply was found to be immediately effective (Fig. 1.4b). Taken together, I conclude that B deprivation-induced death in tobacco BY-2 cells is unlikely to be PCD.

It has been reported that hydrogen peroxide (H_2O_2) can induce different responses in tobacco BY-2 cells depending on the dose and duration of exposure (de Pinto et al. 2006). Under a threshold value, H_2O_2 induces a modest rise in cellular antioxidant capacity, such as the GSH pool and APX activity, as a defense mechanism against stress. On the other hand, higher amounts of H_2O_2 lead to depletion of antioxidant capacity and either PCD or cell necrosis; PCD is triggered if a higher amount of H_2O_2 is given in a single pulse, whereas cell necrosis occurs under more prolonged exposure to H_2O_2. In this study, I did not find any marked decrease in antioxidant enzyme activities upon B deprivation (Fig. 1.5a). I also found that the extracellular H_2O_2 concentrations were not significantly different between +B and –B cultures (data not shown). These data suggest that, in tobacco BY-2 cells, the B deprivation-triggered

overproduction of ROS is not high enough to induce prompt cell death. In fact, the death of –B cells developed rather slowly (Fig. 1.1a), suggesting a low but continuous production of ROS. In this regard, however, I cannot exclude the possibility that B deprivation may induce more acute damage in some cases. Cakmak and Römheld (1997) reported a marked decrease in the content of ASC and non-protein SH compounds in B-deficient sunflower plants, which was not observed in this study. I assume that the discrepancy reflects the severity of oxidative damage imposed on the cells. In plants, ROS are inevitably produced in chloroplasts during photosynthesis (Foyer et al. 1994). Thus more ROS may accumulate in photosynthesizing green leaves than in heterotrophic cultured tobacco cells, when the redox balance is disturbed under B deficiency.

In this study I have demonstrated the involvement of oxidative damage in the final stage of B deficiency. What remains to be clarified is why B deficiency leads to the ROS overproduction. Considering that > 98% of B in tobacco BY-2 cells localizes in the cell wall (Matoh et al. 1992), and that B deprivation alters the physical properties of squash root cell walls within minutes (Findeklee et al. 1997; Goldbach et al. 2001), it would be reasonable to assume that the B deprivation response begins with aberrations in the cell wall structure. At least two hypotheses could explain the subsequent events. First, when cell growth is arrested due to the inability to organize a normal cell wall, energy consumption would be decreased. This would lead to an over-reduction of the mitochondrial electron transport chain, which favors the generation of superoxide radical anions (Purvis 1997). A second possible mechanism is overaccumulation of ROS that have been produced as a signal for the disturbed cell wall structure. Ryden et al. (2003) demonstrated that the B-RG-II complex contributes significantly to maintaining the tensile strength of the cell wall, in studies using the *Arabidopsis* mutant *mur1* with a defective RG-II structure. Their finding suggests that if the B-RG-II complex is not formed properly due to B deficiency, the cell wall would become weaker and less resistant to turgor pressure. In turn, this could trigger Ca^{2+} influx through stretch-activated Ca^{2+} channels in the plasma membrane (Nakagawa et al. 2007), and thereby activate the generation of ROS as signaling molecules (Lecourieux et al. 2006). Similar events may also occur in deprivation experiments. Since B-RG-II complexes are highly stable in vitro (Kobayashi et al. 1997), existing B-RG-II bonding in pectic polysaccharides may be retained even when B is removed from the medium. However, the mechanical strength of squash root cell walls is reduced within minutes after B deprivation (Findeklee et al. 1997; Goldbach et al. 2001), suggesting that significant changes in cell wall

structure occur upon B deprivation. This may be either because the B-RG-II bonding in vivo is less stable than in vitro, or because a failure in cross-linking newly secreted polysaccharides is critical. I assume that generation of ROS as a signal is a more plausible hypothesis because Kobayashi et al. (2004) previously found that several ROS-responsive genes are induced within 30 min after B deprivation in tobacco BY-2 cells. Such a rapid induction is more likely to be triggered by the ROS produced as a signal, rather than the ROS resulting from reduced energy consumption.

Interestingly, the biochemical changes I observed in the B-deprived tobacco cells are similar to those in the aluminum-treated tobacco cells (Yamamoto et al. 2002), in which downstream oxidative stress plays a crucial role in inhibiting growth, and BHA effectively suppresses the damage. Given that the primary target of aluminum toxicity is the cell wall (Ma et al. 2004), these events may represent a general cellular response to the defects in the cell wall. A plant cell wall is a dynamic and responsive structure which is important for the symplast, not only as a mechanical support but also as an interface with the external environment (Hoson 1998). The idea is now emerging that cell walls can generate stress signals that induce cell death. For example, the *Arabidopsis* mutant *cev1* has reduced cellulose content and constitutively expresses stress- and defense-responsive genes (Ellis et al. 2002), and the inhibition of cellulose synthesis by thaxtomin A or isoxaben induces PCD in *Arabidopsis* (Duval et al. 2005). Studies on the responses of tobacco cells to B deprivation will contribute to a better understanding of the mechanism by which the symplast senses defects in the cell wall, and are conducted in the following chapters of this study.

Chapter 2

Analysis of Adaptive Responses to Boron Deprivation

2.1 Introduction

In the previous chapter, I have revealed that oxidative damage is the major cause of cell death induced by B deprivation. Increased content of antioxidants such as ASC and GSH was detected in –B cells to avoid oxidative damage (Koshiba et al. 2009; Chapter 1). Antioxidant gene expression was also up-regulated in –B cells within 30 min (Kobayashi et al. 2004). Camacho-Cristóbal et al. (2008) reported that the expression of several cell wall-modifying enzymes is down-regulated after 6 and 24 h of B deprivation, which could alter the cell wall loosening, resulting in cell elongation (Cosgrove 1999). For instance, the decrease of several xyloglucan endotransglycosylase/hydrolases transcript levels observed under B deficiency (Camacho-Cristóbal et al. 2008) might affect the rearrangement of the xyloglucan cross-linked microfibrillard network with the consequent alteration in the tensile properties of cell walls (Ryden et al. 2003). These data indicated that –B cells exhibited the adaptive responses to oxidative stress and alteration in the tensile properties of cell wall.

In this chapter, I investigated that what kind of gene expression changed in –B cells using 16K cDNA microarray in order to clarify the responses to B deprivation.

2.2 Materials and methods

2.2.1 Cell culture and treatments

Suspension-cultured tobacco cells (*Nicotiana tabacum* L. cv. Bright Yellow-2) were cultured and deprived of B as described in Chapter 1. Cells were collected by filtration under suction at 1, 3, 6, 12 and 36 h after treatment, snap-frozen in liquid nitrogen and stored at –80°C until use.

2.2.2 RNA isolation and microarray analysis

Total RNA was prepared using TRIzol reagent (Invitrogen, Carlsbad, CA, USA) as described in the manufacturer's protocols. The poly(A)-rich RNA fraction was isolated from total RNA using a GenElute mRNA Miniprep Kit (Sigma-Aldrich,. St. Louis, MO, USA) in two subsequent runs of purification following the manufacturer's protocol. The quality of isolated poly(A) RNA was estimated by Bioanalyzer. One μg of the RNA was labeled using SuperScript II reverse transcriptase (Invitrogen), random 9-mer primers, poly(A)-specific poly (dT) primers, and Cy-3/Cy-5-labeled dCTP nucleotides (Amersham Biosciences, Buckinghamshire, UK) and used for single-slide hybridizations. Samples were spiked with control Kanamycin mRNA (Promega, Madison, WI, USA). Quality of the probe was estimated by gel electrophoresis and subsequent fluoroimaging analysis.

Prior to hybridization, the DNA spotted on the microarray slides was immobilized by cross–linking under UV light at 50 mJ cm^2. The slides were prehybridized for 1 h at 55°C in prehybridization buffer [1% bovine serum albumin, 5×saline sodium citrate (SSC) and 0.1% sodium dodecyl sulfate (SDS)] as described (Demura et al. 2002; Matsuoka et al. 2004).

Hybridization of microarrays with Cy-5-labeled sample cDNA and Cy-3-labeled control DNA was performed in ExpressHyb hybridization solution (Clontech, Palo Alto, CA, USA) at 60°C for 4 h as described by Demura et al. (2002) with modification. As Cy-3-labeled control DNA, we used the polylinker sequence located between the M13 forward/reverse or M13 forward/KS reverse primer sites of pGEM-Teasy or pBluescript II KS+, respectively. The hybridized slides were washed in SSC/SDS buffer solutions at 55°C (final wash in 0.1× SSC and 0.1% SDS), briefly rinsed with water, and dried by centrifugation. The Cy-5- (sample signal) and Cy-3- (control signal) labeled signals were obtained by scanning with a GenePix 4000A microarray scanner (Molecular Dynamics). The scans were subsequently analyzed by the MicroArray Suite iplab program (Scananalytics, BD Biosciences, Rockville, MD, USA).

Raw signal data were first processed by subtraction of respective background values. Ratio of (Cy-5-labeled cDNA signal)/(Cy-3-labeled vector control signal) after background correction was used as a signal intensity for the spot. Signals from –B cells were divided with that from +B cells and the $\log_2$ values of the ratio were calculated. As the slides have duplicate spot for each

cDNA, an average for the two $\log_2$ values was calculated. Analysis was carried out with two independent biological replicates.

2.2.3 Mitochondrial Activity

Reduction of MTT

The assay was performed according to Yamamoto et al. (2002). After –B treatment, cells (5 ml aliquots) were added with 250 μg ml^{-1} 3-(4,5-dimethylthiazol-2-yl)-2,5-diphenyltetrazolium bromide (MTT; Dojindo Laboratories, Kumamoto, Japan), and the suspension was shaken at 130 rpm for 1 h at 25°C in darkness. Cells were then harvested, resuspended in 10 ml of isopropanol containing 40 mM HCl, and vortexed vigorously to dissolve the formazan produced by the reduction of MTT. Cells were removed by centrifugation, and formazan was determined spectrophotometrically at 590 nm.

Uptake of rhodamine123 (Rh123)

The assay was performed according to Yamamoto et al. (2002) with some modifications. After –B treatment, cells (1 ml aliquots) were added with Rh123 (2 μg ml^{-1}; Molecular Probes, Eugene, OR), and the suspension was incubated for 60 min at 25°C in darkness. Uptake of Rh123 into mitochondria was examined under a fluorescence microscope (BX-51, Olympus, Tokyo, Japan) with a 460-495 nm excitation filter and a 510 nm barrier filter.

2.3 Results and discussion

Three-day-old tobacco cells were washed with and transferred to standard or B-free culture medium and continued to be cultured. Hereafter these cells were referred to as +B or –B cells, respectively. Transcriptome analysis was done with two independent biological replicates using custom microarray of tobacco BY-2 ESTs (Gális et al. 2006). In each experiment, I compared –B and +B signals and picked up ESTs with at least two-fold higher or lower signals at any of the five time points observed (1, 3, 6, 12 or 36 h after –B treatment). The picked up ESTs were

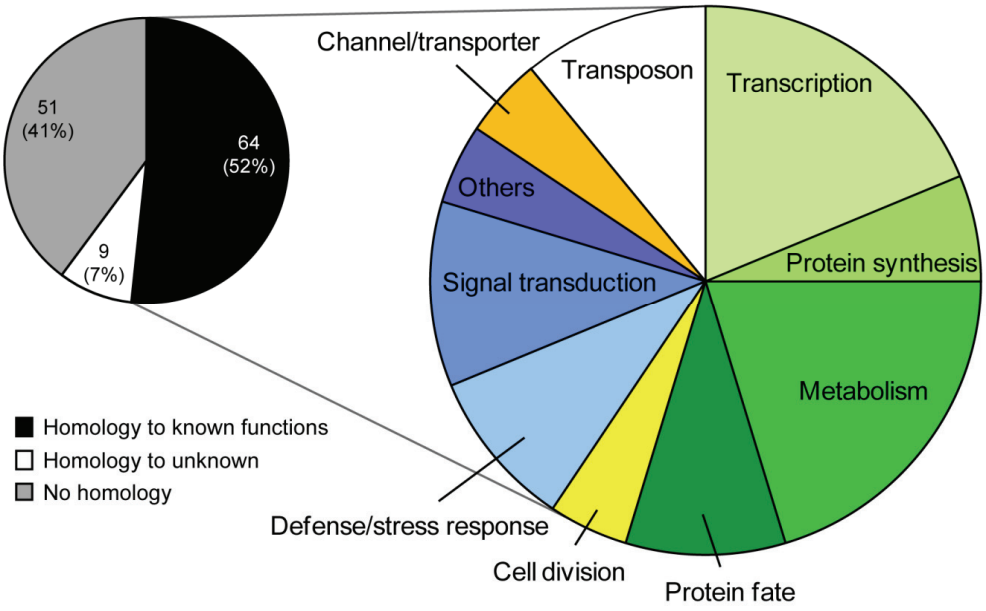

Fig. 2.1 Functional classification of tobacco BY-2 ESTs induced or suppressed by B deprivation. Functions of proteins represented by the identified ESTs were estimated by a BLASTX search. The left graph shows the percentage of ESTs that showed homology to genes with known or predicted functions, that showed homology to genes encoding unknown proteins, or that showed no homology to known genes. The right graph shows the functional distribution of ESTs with known or predicted functions.

further filtered based on whether they were present in both of the lists for two biological replicates. Of approximately 16,000 ESTs included in the array, only 124 ESTs fitted these criteria. BLASTX searches (Altschul et al. 1990) showed that 52% of the identified ESTs were significantly similar [an expected value (E-value) < 1.00 E-4] to at least one protein sequence in the public database, while 48% did not show significant similarity to known proteins (Fig. 2.1 left).

The ESTs identified were classified based on the putative functions (Fig. 2.1 right, Table 2.1). A major fraction of ESTs in Fig. 2.1 and Table 2.1 represent the genes involved in primary cellular process such as transcription, translation and cell metabolism. ESTs representing the

---

Fig. 2.2 Time-dependent changes in expression ratio of ESTs listed in Table 2.1. Each functional group in Table 2.1 was arbitrary assigned to one of five panels to facilitate visualization. Experiment 1 and 2 were independent biological replicates.

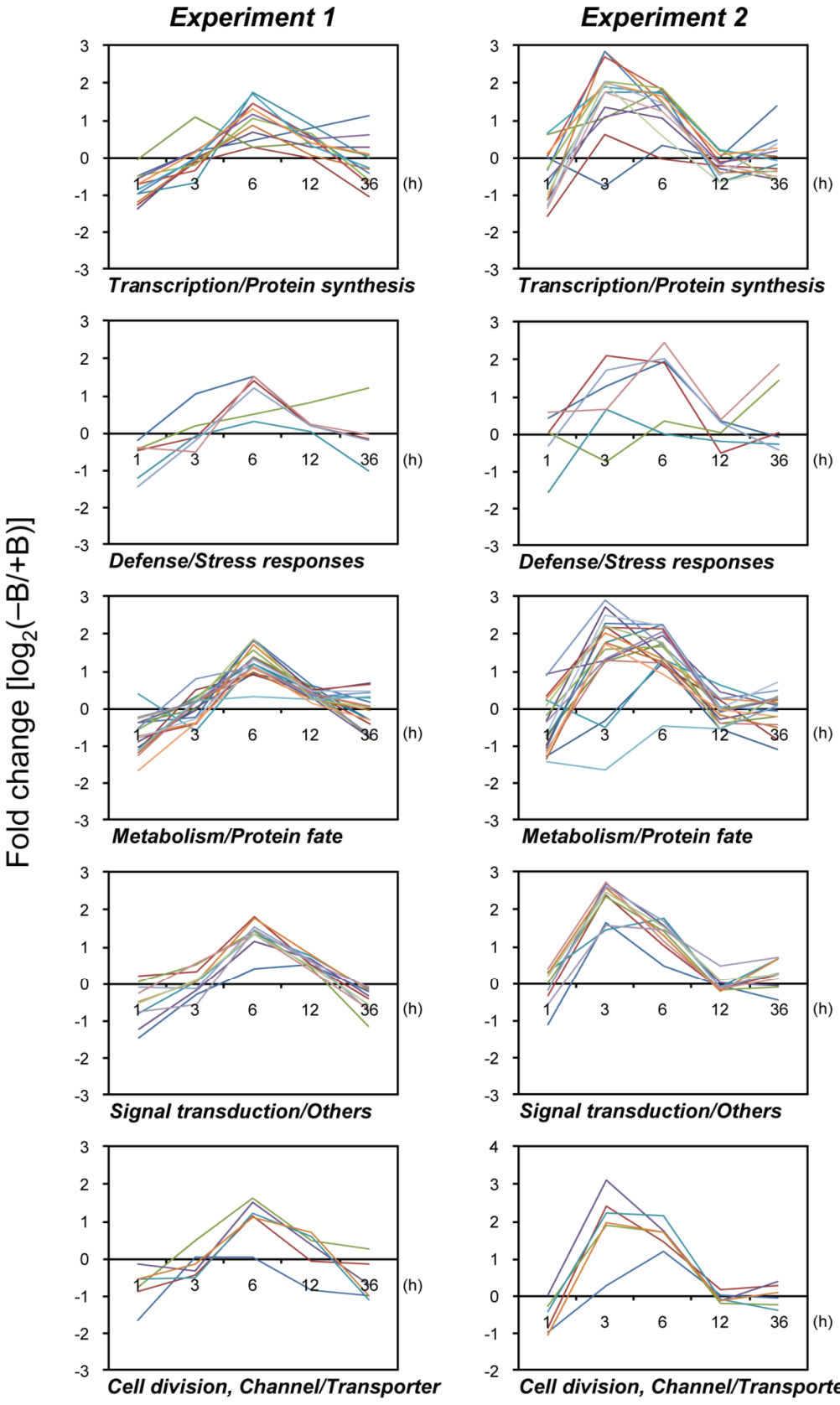
Experiment 1
Experiment 2
Fold change [log2(–B/+B)]
Transcription/Protein synthesis
Defense/Stress responses
Metabolism/Protein fate
Signal transduction/Others
Cell division, Channel/Transporter
1 3 6 12 36 (h)
Time after treatment

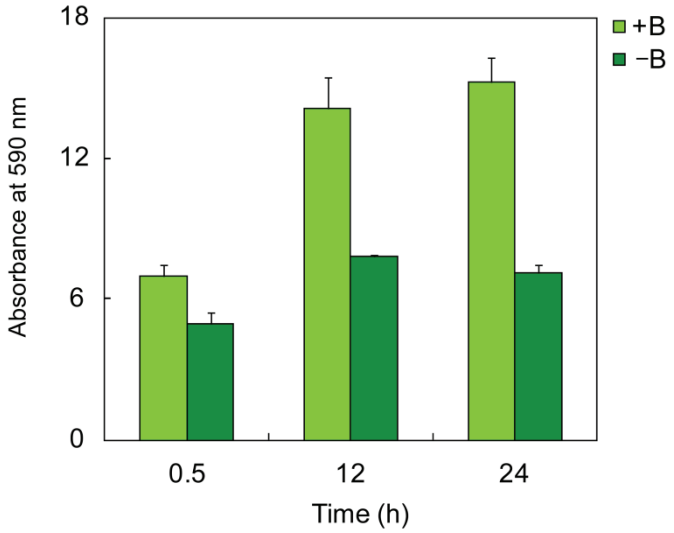

Fig 2.3 Difference of MTT reduction activity between +B and –B cells. The activity was expressed as absorbance of formazan at 590 nm per gram flesh weight of cells.

ubiquitin-proteasome system were also found (Table 2.1). However, no obvious correlation was found between the temporal change in ratio and the functional categories (Fig. 2.2). Rather, almost all genes in the list exhibited a similar trend in –B/+B ratio of expression; when compared to the expression in +B cells, the expression in –B cells was suppressed at first, induced from 3 to 6 h, then converged to a similar level to that in +B cells after 12 h (Fig. 2.2). Although Camacho-Cristóbal et al. (2008) reported that the expression of several cell wall-modifying enzymes is down-regulated at 6 or 24 h after B deprivation in *Arabidopsis* root, no such enzymes were found to be induced in this study. This result might be the cause of change in expression by mechanical stress. In this study, cells were washed by changing their surrounding medium, which was probably stimulating enough to change the expression of mechanical stress-responsive genes. However, since +B cells also got the mechanical stress, the result suggest that, as for changing of gene expression, the effect of B disappearance was not as significant as that of cell washing. These results suggest that cells deprived of B attempted to acclimate to –B stress condition through accelerating their metabolism and/or damage repair system. Although function of about half of the identified ESTs are unknown, none of them was up-regulated at initial stage of deprivation and would not be expected to encode –B

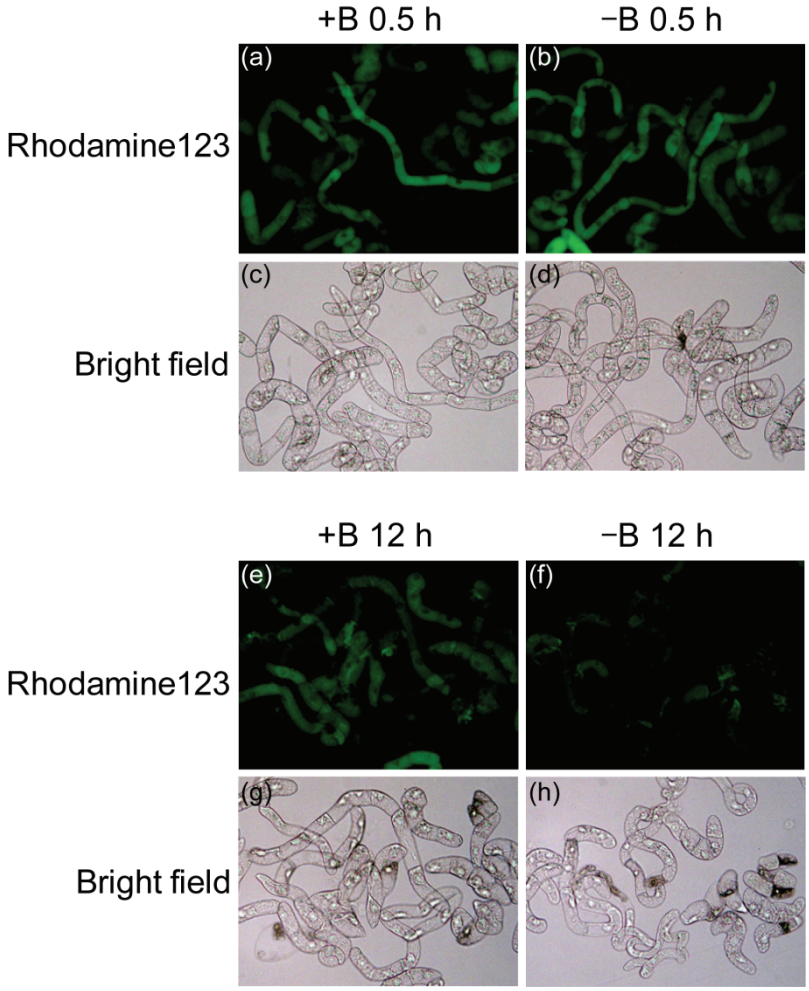

Fig 2.4 Mitochondrial depolarization by B deprivation. Cells with +B (a, c, e, g) or –B (b, d, f, h) were stained with Rh123 and observed 0.5 h **(a-d)** or 12 h **(e-h)** after treatment.

stress-specific factors.

Mitochondrial activities of the cells were monitored by either the formation of formazan from MTT or the uptake of Rh123 into mitochondria. MTT freely enters into cells and is reduced to formazan by the mitochondrial electron transport chain (Slater et al. 1963). Rh123 is taken up into mitochondria depending on the transmembrane electrochemical potential ($\Delta\Psi m$; Kroemer et al. 1998; Scheffler 1999) and therefore serve as a fluorescent probe to identify active mitochondria. MTT reduction in –B cells at 0.5 h was slightly lower than that in +B cells

(Fig. 2.3). In +B cells, MTT reduction increased over time to twice as much as that at 0.5 h, while that in –B cells did not increase markedly (Fig. 2.3). MTT reduction in 12-h –B cells was approximately half of that in corresponding +B cells. The difference was also seen in Rh123 uptake. There was no difference in the fluorescence between +B and –B cells at 0.5 h after treatment (Fig. 2.4a, b). However, the fluorescence from –B cells were much weaker than that from +B cells at 12 h (Fig. 2.4e, f), suggesting that mitochondria was depolarized in –B cells. These data indicate that B deprivation induces mitochondrial dysfunction. It has been reported that mitochondrial dysfunction and significant decrease in ATP level occur in the cells undergoing necrosis (Casolo et al. 2005). As mitochondrial dysfunction and necrosis (Koshiba et al. 2009; Chapter 1) occurred also in this study, it is likely that ATP depletion also occurred. From this estimation, it is conceivable that ATP depletion due to mitochondrial dysfunction under –B condition would suppress gene expression. This may explain why B deprivation-induced cell death proceeds rather slowly, and B resupply immediately suppresses the following cell death (Koshiba et al. 2009).

Table 2.1 Genes differentially expressed in –B and +B cells. List includes the genes whose expression was increased or decreased at least two fold in –B cells compared to +B cells. Fold change indicates $\log_2$(–B/+B) value. Each value is the average of two replicates.

Functional Category	EST ID	Acc. No.	BLAST match				Experiment 1 [Log2(-B/+B)]					Experiment 2 [Log2(-B/+B)]				
			Protein	Organism	Protein ID	E-value	1 h	3 h	6 h	12 h	36 h	1 h	3 h	6 h	12 h	36 h
Transcription	4220	BP132085	Helix-loop-helix DNA-binding	*Medicago truncatula*	ABN06010.1	6.00E-11	-0.03	1.08	0.30	0.41	0.08	0.61	1.05	1.82	0.18	0.03
	9916	BP137239	NsRpoT-B gene for T7 bacteriophage-type single subunit RNA polymerase	*Nicotiana sylvestris*	AB058958.1	2.00E-87	-1.38	0.00	0.68	0.29	0.29	-1.16	1.34	1.06	-0.29	-0.61
	9996	BP137313	F-box family protein	*Populus trichocarpa*	XP_002300142	2.00E-07	-0.95	-0.68	1.76	0.87	0.00	-0.79	1.74	1.77	-0.66	-0.21
	10111	BP137415	bZIP transcription factor BZI-2	*Nicotiana tabacum*	AAK92213	3.00E-37	-1.18	-0.08	0.86	0.07	-0.29	-1.14	2.87	1.51	-0.41	-0.39
	12133	BP527346	Nucleic acid binding / zinc ion binding	*Arabidopsis thaliana*	NP_178215	4.00E-06	-0.98	-0.01	1.47	0.58	-0.41	-0.34	2.84	1.25	-0.21	0.46
	13443	BP528588	MYB-related transcription factor	*Nicotiana tabacum*	BAF80451	2.00E-18	-0.49	-0.18	1.06	0.66	-0.60	-0.29	2.04	1.87	0.21	-0.65
	13540	BP528679	MADS transcriptional factor; STMADS11	*Solanum tuberosum*	AAB94006	4.00E-07	-0.56	0.19	1.15	0.49	0.60	-0.58	1.09	1.41	-0.16	0.17
	14446	BP529544	Histone acetyltransferase complex component	*Populus trichocarpa*	EEF04890	3.00E-23	-0.69	-0.34	1.48	0.56	-0.72	0.04	2.70	1.84	-0.11	0.01
	32170	BP534213	WRKY transcription factor, putative	*Ricinus communis*	EEF28610	4.00E-05	-0.84	-0.05	1.73	0.31	-0.26	0.65	1.92	1.71	0.22	-0.08
	33173	BP534591	HNH endonuclease domain-containing protein	*Arabidopsis thaliana*	NP_190333	6.00E-61	-0.69	0.16	1.33	0.39	0.10	0.11	2.03	1.64	0.07	0.26
	33274	BP534689	Zinc finger protein, putative	*Ricinus communis*	XP_002522447	1.00E-14	-1.75	-0.18	1.89	0.58	-0.36	-0.61	2.54	1.75	0.29	0.09
	35275	BP535435	Myb-like DNA-binding protein, putative	*Solanum demissum*	AAU90342	3.00E-43	-1.73	-0.19	1.61	1.11	-0.06	-1.26	2.50	0.75	0.29	0.01
Protein synthesis	10147	BP137449	CBP20 (Cap-binding Protein)	*Solanum tuberosum*	ACY07775	3.00E-10	-0.18	0.27	1.26	0.48	0.44	-1.29	2.07	1.47	-0.50	0.37
	10546	BP525852	putative leucyl tRNA synthetase	*Arabidopsis thaliana*	CAB77903.1	4.00E-21	0.04	0.33	1.80	0.36	-1.06	-0.71	2.46	1.19	-0.42	0.24
	11872	BP527106	Pentatricopeptide (PPR) repeat-containing protein	*Arabidopsis thaliana*	NP_187753	1.00E-22	-0.68	0.23	1.92	0.26	-0.19	-0.16	2.16	1.92	-0.13	-0.21
	14810	BP529861	Putative RNA-binding protein; 42664-44784	*Arabidopsis thaliana*	AC012680_4	5.00E-47	-1.50	-0.22	0.88	0.22	-0.27	-1.00	1.99	0.57	-0.69	-0.32
Metabolism	9925	BP137248	Hexokinase 2	*Nicotiana tabacum*	AAS60193	3.00E-14	-1.09	0.00	0.92	0.54	-0.34	-1.29	-0.34	1.21	-0.58	-1.10
	10015	BP137326	2-deoxyglucose-6-phosphate phosphatase, putative	*Ricinus communis*	EEF29505	6.00E-24	-1.14	0.45	0.88	0.38	-0.45	-1.00	2.19	1.13	0.21	-0.88
	11580	BP526831	Adenosine-5'-phosphosulfate-kinase	*Catharanthus roseus*	AAG31145	2.00E-32	-0.42	-0.04	1.33	0.53	-0.86	-0.75	1.24	1.73	-0.43	-0.25
	12142	BP527354	NADH dehydrogenase subunit 5	*Nicotiana tabacum*	AAA84685	2.00E-62	-0.93	-0.09	1.77	0.41	0.65	-0.34	2.70	1.36	-0.32	0.00
	13483	BP528627	Acetyl CoA carboxylase	*Glycine max*	AAA75528	4.00E-06	-0.60	0.28	1.17	0.43	-0.36	-0.84	1.75	2.24	-0.08	0.22
	14051	BP529165	Mitochondrial glycine decarboxylase complex H-protein	*Populus tremuloides*	ABO61731	6.00E-28	-1.23	0.11	0.93	0.22	-0.08	-1.37	1.76	1.23	-0.21	-0.53
	14107	BP529217	Serine carboxypeptidase S10 family protein	*Arabidopsis thaliana*	NP_850035	8.00E-07	-0.42	-0.29	1.81	0.59	0.12	-1.08	2.26	2.22	0.04	-0.08
	14954	BP529981	Mitochondrial fission protein	*Arabidopsis thaliana*	BAG66280	1.00E-08	-0.82	-0.46	1.32	0.46	0.61	0.31	2.16	2.10	-0.04	0.19
	31119	BP533799	CYP72A55v1 (cytochrome P450)	*Nicotiana tabacum*	ABC69392	4.00E-14	-0.59	0.24	1.54	0.31	-0.75	-0.22	1.57	1.64	-0.06	0.23
	31127	BP533807	Threonine deaminase	*Nicotiana attenuata*	AAX22214	4.00E-09	-0.40	0.16	1.03	0.24	-0.81	0.90	1.26	1.93	0.42	0.06
	31337	BP534005	UP-9A (sulpher metabolism)	*Nicotiana tabacum*	ABF06706	5.00E-28	0.34	-0.62	1.15	0.30	0.24	0.21	-0.53	1.30	0.60	0.09
	33324	BP534738	Acyl-CoA-binding protein	*Ricinus communis*	XP_002510117	7.00E-04	-0.77	-0.40	1.69	0.35	-0.01	0.23	2.00	1.32	0.25	0.13
	35355	BP535511	putative lipid transfer protein	*Solanum tuberosum*	BAC23052.1	9.00E-07	-0.57	0.74	1.08	0.29	0.38	0.86	2.87	1.68	0.25	0.45
Protein fate	10055	BP137364	Protein ariadne-1, putative	*Ricinus communis*	EEF28857	6.00E-19	-1.29	0.13	1.05	0.36	0.01	-1.14	1.26	1.18	-0.43	-0.47
	10193	BP137495	Peptidylprolyl isomerase (Cyclophilin)	*Arabidopsis thaliana*	BAB10690	2.00E-35	-0.32	0.12	1.81	0.22	0.00	0.05	2.20	1.76	-0.58	0.32
	11366	BP526629	COP1 (ubiquitin ligase)-interacting protein-related	*Arabidopsis thaliana*	NP_568624	5.00E-06	-0.26	0.14	1.31	0.37	-0.76	-0.37	1.30	2.03	-0.12	0.27
	13755	BP528865	Circadian clock-associated FKF1	*Glycine max*	ABD28287	7.00E-16	-1.14	0.16	0.29	0.22	0.29	-1.45	-1.67	-0.48	-0.58	0.04
	14192	BP529302	RING-H2 finger protein ATL3K, putative	*Ricinus communis*	EEF39071	2.00E-19	-1.70	-0.40	1.10	0.08	-0.36	-1.24	1.72	0.92	-0.06	-0.22
	14958	BP529985	ATL8; protein binding / zinc ion binding	*Arabidopsis thaliana*	NP_177767	2.00E-34	-0.84	-0.32	1.27	0.44	0.43	-0.70	2.48	2.20	-0.02	0.69
Cell Division	5386	BP133153	Kinesin-like polypeptides 2	*Nicotiana tabacum*	BAB40701	2.00E-09	-1.66	0.00	0.00	-0.87	-1.00	-1.00	0.26	1.16	0.00	-0.08
	11732	BP526973	SEC14-like protein	*Oryza nivara*	ACN85154	2.00E-59	-0.92	-0.46	1.12	-0.09	-0.17	-0.89	2.38	1.41	0.14	0.24
	31364	BP534031	Nucleosome assembly protein 1-like protein 4	*Nicotiana tabacum*	CAD27463	4.00E-04	-0.79	0.46	1.61	0.46	0.24	-0.31	1.86	1.67	-0.22	-0.27
Defense/Stress response	1870	BP129960	Catalase (EC 1.11.1.6) CAT-2	*Zea maize*	A55092	6.00E-07	-0.22	0.99	1.49	0.16	-0.20	0.40	1.25	1.89	0.33	-0.13
	10093	BP137402	Beta-D-glucan exohydrolase	*Nicotiana tabacum*	BAA33065	3.00E-28	-0.52	-0.15	1.35	0.13	-0.21	0.00	2.05	1.88	-0.56	0.00
	10131	BP137435	api2 (GST, AI-induced) *par*B	*Nicotiana tabacum*	BAA06150	4.00E-12	-0.49	0.16	0.47	0.79	1.15	-0.01	-0.77	0.32	-0.02	1.40
	14188	BP529298	NBS resistance protein	*Populus trichocarpa*	XP_002326564	3.00E-05	-1.25	-0.10	0.27	0.00	-1.04	-1.59	0.62	-0.06	-0.23	-0.31
	30273	BP533582	Aspartic proteinase nepenthesin-1 precursor, putative	*Ricinus communis*	XP_002514026	9.00E-46	-1.49	-0.24	1.15	0.17	-0.25	-0.34	1.65	1.98	0.25	-0.49
	35169	BP535330	Kunitz trypsin inhibitor	*Nicotiana tabacum*	ACL12055	2.00E-57	-0.43	-0.56	1.49	0.20	-0.08	0.53	0.62	2.41	0.35	1.82
Signal transduction	10016	BP137327	SWP1	*Arabidopsis thaliana*	AF466359_1	7.00E-11	-1.48	-0.30	0.37	0.52	-0.24	-1.13	1.63	0.48	-0.08	-0.47
	10580	BP525886	Ptm1, putative	*Ricinus communis*	EEF33684	8.00E-10	0.21	0.30	1.79	0.51	-0.44	-0.37	2.37	1.00	-0.16	0.24
	11841	BP527075	Putative ethylene receptor	*Nicotiana tabacum*	AAF20093	9.00E-22	0.03	0.52	1.40	0.42	-1.15	0.00	2.34	1.39	-0.20	-0.13
	13433	BP528578	Ser/Thr protein kinase	*Solanum chacoense*	ACD75053	3.00E-72	-1.26	-0.18	1.12	0.67	-0.34	-0.18	2.67	1.54	0.00	-0.10
	13517	BP528656	Protein phosphatase 2C, putative	*Arabidopsis thaliana*	NP_190715	6.00E-06	-0.83	0.04	1.32	0.75	-0.17	0.29	1.44	1.73	-0.11	0.64
	14461	BP529559	RALF (Rapid ALkalinization Factor) precursor	*Nicotiana tabacum*	AF407278_1	4.00E-26	-0.53	0.04	1.76	0.76	-0.18	0.28	2.57	1.29	-0.24	0.64
	14744	BP529812	Two-component response regulator ARR8, putative	*Ricinus communis*	EEF49566	1.00E-18	-0.13	-0.18	1.50	0.61	-0.74	-0.19	2.62	1.68	-0.13	0.28
Others	10370	BP525684	zinc ion binding	*Arabidopsis thaliana*	NP_566784.1	2.00E-21	-0.28	0.54	1.31	0.33	-0.71	0.37	2.72	1.14	-0.15	0.10
	13214	BP528369	Calcium ion binding protein, putative	*Ricinus communis*	EEF36409	1.00E-34	-0.57	0.08	1.33	0.48	-0.60	0.21	2.44	1.52	0.06	0.23
	14960	BP529987	Calmodulin-binding protein-related	*Arabidopsis thaliana*	NP_181414	3.00E-11	-0.79	-0.57	1.43	0.59	-0.12	-0.60	1.54	1.45	0.45	0.68
Channel/Transporter	11374	BP526637	Multidrug resistance pump, putative	*Ricinus communis*	EEF48574	4.00E-06	-0.17	-0.34	1.49	0.33	-0.71	-0.03	3.05	1.71	-0.17	0.35
	12928	BP528099	Multidrug Resistance associated Protein 1	*Catharanthus roseus*	CAO94660	2.00E-15	-0.59	-0.53	1.20	0.56	-1.13	-0.44	2.17	2.11	-0.13	-0.40
	14436	BP529534	TPK1 (K+ channel)	*Nicotiana tabacum*	ABX60975	4.00E-65	-0.57	-0.18	1.09	0.66	-1.02	-1.06	1.94	1.69	-0.16	0.08
Transposon	9909	BP137232	Polypeptide with a gag-like domain	*Petunia x hybrida*	BAD99219	2.00E-09	-1.51	-0.27	0.77	0.09	-0.42	-1.01	1.70	1.69	-0.29	0.16
	10082	BP137391	Retroelement pol polyprotein-like	*Arabidopsis thaliana*	BAB10790	6.00E-34	-0.68	0.16	1.02	0.31	0.75	0.13	1.88	2.10	0.00	-0.39
	12741	BP527920	Polypeptide with a gag-like domain	*Petunia x hybrida*	BAD99219	3.00E-19	-0.60	-0.10	2.11	0.45	-0.25	-0.42	2.21	1.43	-0.06	-0.18
	12863	BP528038	Retrovirus-related Pol polyprotein	*Nicotiana tabacum*	CAA32025	9.00E-15	-1.82	-0.44	1.15	0.18	-1.18	-1.49	2.17	1.36	-0.05	0.29
	13773	BP528903	Copia-type polyprotein	*Arabidopsis thaliana*	BAB11200	2.00E-22	-1.47	-0.62	0.73	-0.44	-1.57	-1.29	1.16	0.90	-0.63	-0.42
	13816	BP528942	Retrovirus-related Pol polyprotein	*Nicotiana tabacum*	CAA32025	2.00E-25	-1.77	-0.57	0.93	-0.29	-0.81	-1.12	2.07	0.08	-0.19	-0.53
	33108	BP534528	LTR retrotransposon like protein	*Arabidopsis thaliana*	CAB79159	1.00E-23	-0.63	0.07	1.52	0.44	-1.08	0.06	2.88	2.24	0.29	-0.07

$\log_2$(-B/+B)

2

-2

Functional Category	EST ID	Acc. No.	BLAST match				Experiment 1 [Log2(-B/+B)]					Experiment 2 [Log2(-B/+B)]				
			Protein	Organism	Protein ID	E-value	1 h	3 h	6 h	12 h	36 h	1 h	3 h	6 h	12 h	36 h
Unknown	946	BP129116	hypothetical protein	*Vitis vinifera*	CAN62820	5.00E-05	0.63	0.56	1.24	-0.04	-0.07	-0.27	0.12	1.75	1.08	-0.50
	11277	BP526547	hypothetical protein	*Arabidopsis thaliana*	NP_173097.2	9.00E-41	-1.10	-0.15	1.02	0.07	0.13	-0.76	2.03	1.34	-0.11	-0.03
	11734	BP526975	hypothetical protein	*Ricinus communis*	EEF49378	6.00E-16	-1.29	-0.49	1.67	-0.09	0.09	-0.08	2.45	1.70	0.21	0.08
	12784	BP527963	hypothetical protein	*Vitis vinifera*	XP_002273501	6.00E-24	-0.78	-0.13	1.39	0.60	0.07	-0.10	2.60	2.06	-0.20	-0.27
	13189	BP528349	hypothetical protein	*Vitis vinifera*	CAO70793	3.00E-24	-0.69	0.13	1.36	0.54	-0.35	-0.26	2.94	2.28	-0.51	0.16
	13233	BP528387	hypothetical protein	*Ricinus communis*	XP_002520162	4.00E-15	-0.76	0.30	1.27	0.40	0.21	-0.70	1.78	1.97	-0.28	0.47
	22189	BP530553	hypothetical protein	*Oryza sativa*	EAZ28420	3.00E-19	-1.74	0.00	-0.15	-0.47	-0.87	-1.68	-0.92	1.74	0.12	0.10
	30118	BP533429	hypothetical protein	*Vitis vinifera*	CAN77047	4.00E-17	-0.60	1.06	1.66	0.16	-1.45	-0.48	1.67	1.36	-0.15	-0.10
	31334	BP534002	hypothetical protein	*Vitis vinifera*	XP_002265506	3.00E-23	0.50	0.09	1.71	0.45	-0.36	-0.99	2.19	1.83	0.43	0.73
No homology	648	BP128842	No hit				0.00	0.24	1.16	0.08	0.25	0.10	-0.15	1.31	-0.25	-0.74
	1341	BP129475	No hit				-0.05	1.33	0.67	-0.21	1.00	0.16	1.25	1.73	0.31	-0.58
	1525	BP129648	No hit				0.55	1.02	0.97	0.37	0.16	-0.04	1.29	1.65	0.40	-0.50
	4009	BP131896	No hit				0.18	1.44	0.45	0.30	0.32	0.79	1.17	1.66	0.13	0.23
	4064	BP131949	No hit				-0.03	1.09	0.45	0.41	-0.24	-0.40	1.18	1.94	-0.20	-0.18
	4347	BP132200	No hit				0.00	-0.42	1.25	0.14	0.05	0.24	-0.97	1.41	-0.53	-0.22
	5284	BP133059	No hit				-1.67	-0.29	0.21	-1.40	-1.00	-1.00	0.50	0.66	0.50	-1.00
	6585	BP134232	No hit				-0.50	0.40	1.27	0.32	0.09	0.06	0.63	1.09	-0.20	0.49
	9290	BP136681	No hit				0.35	-0.05	0.34	0.24	2.47	-0.04	0.08	1.07	0.83	2.59
	9859	BP137188	No hit				-1.26	-0.27	0.41	0.24	-0.40	-1.21	1.39	0.06	-0.15	-0.79
	9864	BP137193	No hit				-1.54	0.12	0.57	0.25	-0.26	-1.25	1.48	1.12	0.20	-0.66
	9887	BP137215	No hit				-0.77	-0.24	1.76	0.61	0.64	-0.05	2.10	2.14	-0.29	0.52
	9894	BP137222	No hit				-0.68	-0.08	1.26	0.43	0.46	-1.24	2.00	1.59	-0.29	0.21
	9895	BP137223	No hit				-0.63	-0.08	1.72	0.81	0.39	-1.16	2.29	1.52	-0.21	0.50
	9930	BP137253	No hit				-0.75	-0.17	1.24	0.48	-0.31	-0.08	2.06	1.61	-0.10	0.00
	9938	BP137260	No hit				-0.95	0.39	1.53	0.31	-0.06	-0.88	2.27	1.56	-0.17	0.29
	9959	BP137278	No hit				-1.60	-0.05	0.70	0.14	-0.35	-1.61	1.14	0.66	-0.50	-1.02
	9960	BP137279	No hit				-1.63	0.15	0.60	0.14	-0.12	-1.61	0.81	0.62	-0.71	-0.93
	9962	BP137281	No hit				-1.57	0.22	0.81	0.09	-0.20	-1.29	2.51	0.85	0.11	-0.37
	9971	BP137289	No hit				-1.26	-0.10	0.94	0.42	0.08	-1.45	1.74	1.26	-0.29	0.08
	9977	BP137295	No hit				-1.25	-0.95	0.57	0.21	-0.21	-1.33	-0.18	0.25	0.48	-0.20
	9982	BP137300	No hit				-0.75	-0.36	1.35	0.57	0.37	-0.52	1.89	1.34	-0.24	0.11
	10044	BP137354	No hit				-0.38	0.10	1.39	0.42	0.11	0.29	1.95	1.49	-0.29	0.13
	10047	BP137357	No hit				-0.42	-0.23	1.49	0.37	-0.11	0.00	1.70	2.28	-0.21	0.37
	10048	BP137358	No hit				-0.67	-0.12	1.15	0.69	-0.20	0.29	2.04	1.32	-0.40	0.24
	10052	BP137361	No hit				-1.30	-0.21	0.87	0.16	-0.45	-1.40	1.00	0.71	-0.16	0.11
	10149	BP137451	No hit				-1.09	0.36	0.34	0.38	0.00	-1.48	0.78	0.47	-0.48	-0.29
	21167	BP530177	No hit				-1.55	-0.44	-0.46	-0.14	-0.45	-1.14	-0.40	1.35	-0.08	-0.20
	23360	BP531087	No hit				-1.90	-0.07	-0.41	-0.96	0.01	-1.55	0.26	1.51	0.47	-0.04
	24177	BP531283	No hit				-1.57	-0.29	0.05	-1.37	-0.24	-1.21	0.25	1.25	-0.32	0.34
	24182	BP531288	No hit				-1.64	-0.13	0.09	-0.39	0.12	-1.29	-0.45	1.12	0.26	-0.06
	25188	BP531664	No hit				-1.36	0.00	0.02	-1.41	-0.07	-1.36	0.01	1.40	0.07	0.39
	26181	BP532020	No hit				-1.25	0.29	-0.14	0.38	0.26	-1.98	-0.93	0.42	0.14	0.34
	29119	BP533067	No hit				-1.54	0.56	-0.41	-0.57	-0.21	-2.60	0.69	1.22	0.04	0.15
	29371	BP533304	No hit				-1.45	0.48	-0.23	-0.12	0.50	-1.70	0.30	0.17	0.08	0.77
	30112	BP533423	No hit				0.08	0.02	1.62	0.04	-1.17	0.10	1.90	1.62	-0.14	0.02
	30237	BP533546	No hit				-0.98	0.39	1.69	0.04	-0.30	0.43	2.02	1.76	0.25	0.41
	31218	BP533897	No hit				-1.18	0.05	1.27	-0.24	-0.76	-0.29	1.65	1.55	0.19	0.22
	33221	BP534638	No hit				-0.79	0.20	1.63	-0.20	-0.25	-0.35	1.11	1.21	0.31	0.46
	33347	BP534761	No hit				-0.70	-0.20	1.72	0.47	0.45	-0.40	1.99	1.83	0.30	-0.04
	33360	BP534774	No hit				-0.64	-0.05	2.20	0.50	0.57	0.55	1.66	1.78	0.13	0.06
	34047	BP534840	No hit				-1.65	-0.18	0.95	0.00	-0.42	-2.90	1.01	0.57	-0.16	0.22
	34130	BP534921	No hit				-0.94	-0.16	1.06	0.35	-0.64	0.98	1.36	1.40	0.45	0.02
	34176	BP534967	No hit				-0.74	0.15	1.29	-0.03	0.81	0.42	2.41	2.07	0.16	-0.03
	34189	BP534980	No hit				-0.35	0.19	1.15	0.51	0.16	0.75	1.14	1.17	0.19	0.20
	34191	BP534982	No hit				-0.44	0.08	1.43	0.56	0.32	0.75	1.89	1.42	0.11	0.35
	34305	BP535094	No hit				-0.64	0.02	1.04	0.46	-0.56	0.43	1.04	1.26	0.46	-0.06
	34339	BP535127	No hit				-0.69	0.44	2.04	0.30	0.11	0.91	0.12	1.69	0.36	0.24
	34383	BP535168	No hit				-0.07	-0.56	1.81	0.85	0.35	-0.54	1.10	1.80	-0.06	-0.03
	35161	BP535322	No hit				-0.63	0.79	1.53	0.26	0.22	1.46	1.68	1.41	0.37	0.10
	35384	BP535535	No hit				-0.42	-0.15	1.31	0.79	-0.04	-0.66	1.33	1.35	0.02	0.02

Chapter 3

Analysis of Early Responses to Boron Deprivation

3.1 Introduction

In Chapter 2, I have shown that gene expression changes occurred within 1 h after B deprivation. Kobayashi et al. (2004) reported that oxidative stress-responsive genes were up–regulated within 30 min in cells deprived of B. Considering that > 98% of B in tobacco BY-2 cells is localized in the cell wall (Matoh et al. 1992), and that B deprivation could alter the physical properties of cell wall within minutes (Findeklee et al. 1997; Goldbach et al. 2001), it is likely that the cells immediately perceive the disappearance of B through a physical change in cell wall. However, the actual mechanism is not known yet.

In this chapter, I analyze the early responses of tobacco cells to B deprivation with the aim of clarifying the mechanism by which cells quickly perceive the disappearance of B, paying attention to a possible involvement of the cell wall.

3.2 Materials and methods

3.2.1 Cell culture and treatments

Suspension-cultured tobacco BY-2 cells (*Nicotiana tabacum* L. cv. Bright Yellow-2) were cultured and deprived of B as described (Chapter 1). For La^{3+} or Gd^{3+} treatment, phosphate was omitted from the medium to avoid precipitation. $LaCl_3$ or $GdCl_3$ was diluted from 1.5 M aqueous stock solution to a final concentration of 1.5 mM. For Ca^{2+} overdose experiment, cells were preincubated for 1 h in a standard culture medium supplemented with 30 mM $CaCl_2$, then washed with and transferred to a standard or B-free culture medium. For hyperosmotic experiment, cells were washed with and transferred to a standard or B-free culture medium

supplemented with 0.4 M mannitol.

3.2.2 Semi-quantitative RT–PCR analysis

Semi-quantitative RT–PCR analysis was performed as described (Chapter 1). The primer sets used are listed in Table 3.1.

3.2.3 Intracellular Ca^{2+} measurement

Aequorin was reconstituted by incubating 3-d-old apoaequorin-expressing tobacco cells with 2.5 μM native coelenterazine in the culture medium in darkness overnight. Luminescence was measured with GloMax 96 Microplate Luminometer (Promega, Madison, WI, USA). A 100 μl aliquot of cell suspension was transferred to 96-well microplate, and the medium was pipetted off. Cells were washed twice with low Ca (20 μM) medium with or without B, and resuspended in 300 μl of the same medium. The microplate containing the cell suspension was set in the luminometer chamber, and left at 25°C for 5 min. Twenty-five microliter of 39 mM $CaCl_2$ was then injected to the suspension. Luminescence measuring was started 1 min before Ca^{2+} injection and done at 1-s intervals.

3.2.4 Determination of SA contents

Cells were harvested by vacuum filtration and were ground in liquid nitrogen with a mortar and pestle. A 1 g aliquot of the powder was vigorously mixed with 2 ml of 90% (v/v) methanol containing 1 μg of *o*-anisic acid (AA) as an internal standard, and centrifuged at 12,000×g for 5 min at 4°C. The pellet was reextracted with 2 ml of methanol. The extracts were combined and filtered through a 0.45-μm cellulose acetate membrane filter (Millipore Corporation, Bedford, MA). The filtrate were added with 2 μl of 1 M NaOH and evaporated to near dryness using a rotary evaporator. The condensed extract and two subsequent washings of the flask using 1 mM NaOH (0.4 ml each) were pooled and cleaned by passing a Sep-Pak Plus C_{18} cartridge (Waters, Milford, MA, USA) preconditioned with 1 mM NaOH. The flow-through and the washing of the cartridge with 5 ml of 1 mM NaOH were pooled, acidified with 1 ml of 1 M HCl, and left

for 30 min at 25°C. The solution and the washing of the container with 10 mM HCl were applied to a Sep-Pak Plus C_{18} cartridge again to collect undissociated SA on the column. SA was eluted from the cartridge with 100% methanol, evaporated to dryness using rotary evaporator and CENTRIVAP CONSOLE concentrator (LABCONCO Corp., Kansas City, MO), and reconstituted in 100 µl of 80% methanol. The solution was filtered through a 0.20 µm filter (Millipore) to remove any particulate materials. The SA and AA were quantified using liquid chromatography–mass spectrometry with an API3000 LC/MS/MS system (Applied Biosystems, Foster City, CA) equipped with an electrospray ionization interface used to generate negative ions. The SA and AA were separated on a reversed-phase column (Mightysil RP-18 GP 3 µm, 4.6×150 mm) at 40°C with a linear gradient of 25 to 35% (v/v) acetonitrile in 0.1% (v/v) formic acid in 10 min at a flow rate of 0.2 ml min-1 for SA, or 15 to 50% (v/v) acetonitrile in 0.1% (v/v) formic acid in 10 min for AA. Quantification was performed by multiple reactions monitoring of the deprotonated precursor ion and the related product ion for SA or AA. The mass transitions (Q1/Q3) used for SA and AA were *m/z* 137/93 and 151/107, respectively.

3.3 Results and discussion

To gain insights into the mechanism for B deprivation responses of plants, I investigated immediate-early changes in gene expression in B-deprived tobacco BY-2 cells, with which I have characterized the B deprivation-induced cell death (Chapter 1). Cells were washed with either a standard or B-free culture medium, and then cultured in the same medium (hereafter referred to as +B or –B cells, respectively). Using semi-quantitative RT-PCR analyses, I examined whether known immediate-early stress-responsive genes of tobacco were differentially expressed between +B and –B cells at 1 h after treatment. The results are shown in Fig. 3.1.

TOGT was included in the analysis as known –B-responsive gene (Kobayashi et al. 2004). Besides *TOGT*, the following genes were induced in –B cells: phenylalanine ammonia-lyase (*PAL*; Pellegrini et al. 1994), an NPR1/NIM1-interacting protein (*NIMIN2a*; Weigel et al. 2001), ethylene-responsive element binding protein (*EREBP1*; Horvath et al. 1998), mitochondrial alternative oxidase (*AOX*; Maxwell et al. 1999), wound-inducible protein kinase (*WIPK*; Seo et

Table 3.1 Primers used for semi-quantitative RT-PCR analyses

Gene name	Accession no.	Primers used
TOGT	U32643	5'-TCATGGCACAAGCTTCTTTG-3' 5'-ACGTAAACGACGGAACTTGG-3'
PAL	AB008199	5'-GCACAAAATGGTCACCAAGAAA-3' 5'-AAGCCATTGGGGCGACGTTCTA-3'
NIMIN2a	AF057379	5'-AGGCATGAGAGAAAAAGTGC-3' 5'-TAACCTCCAGGATCTTCACC-3'
EREBP1	AF057373	5'-GGAAATTGTGGTTTCTCCAG-3' 5'-AGCTGAACTATTTTCCGACG-3'
AOX	S71335	5'-CACCAATGATGTTGGAAACAGTG-3' 5'-ATACCCAATTGGTGCTGGAG-3'
WIPK	D61377	5'-TGGCTGATGCAAATATGGGTGCCG-3' 5'-GGAAAGTAGATACTCCAGATCA-3'
KED	AB009883	5'-GATGAAGAGGGTCAGAAGAAGGA-3' 5'-GGAAGGGAAAGGTATACACAACG-3'
WIZZ	AB028022	5'-TGCAAGAAACCTAGAGAAGAGCA-3' 5'-CATGATATCGCCTTTTGCTACTG-3'
HIN1	AB091429	5'-CCCTTCCATTCCGCCACCAGCAAAATCC-3' 5'-CTACCAATCAAGATGGCATCTGGTTTCC-3'
ChitIV	AB267862	5'-AGACTGCCCTGTGGTATTGG-3' 5'-TGGGTGCTAACAAGTGAGA-3'
ACT	AB158612	5'-AAGGTTACGCCCTTCCTCAT-3' 5'-GCCACCACCTTGATCTTCAT-3'

al. 1999), a wound-inducible gene with unknown function (*KED*; Hara et al.2000a), a wound-responsive leucine zipper zinc finger protein (*WIZZ*; Hara et al. 2000b), a harpin-induced protein (*HIN1*; Gopalan et al. 1996), and a class IV chitinase (*ChitIV*; Shinya et al. 2007) (Fig. 3.1a, lanes +B and –B). The expression of *PR1a*, *PR1b*, *PR2a*, and *PR2b* were not different between the treatments at this time point (data not shown).

Rapid change in gene expression upon short-term nutrient withholding has been reported for phosphorus (P), potassium (K) and iron (Fe) in tomato plants (Wang et al. 2002). The authors found that the deprivation of these three plant nutritional elements induced the same putative

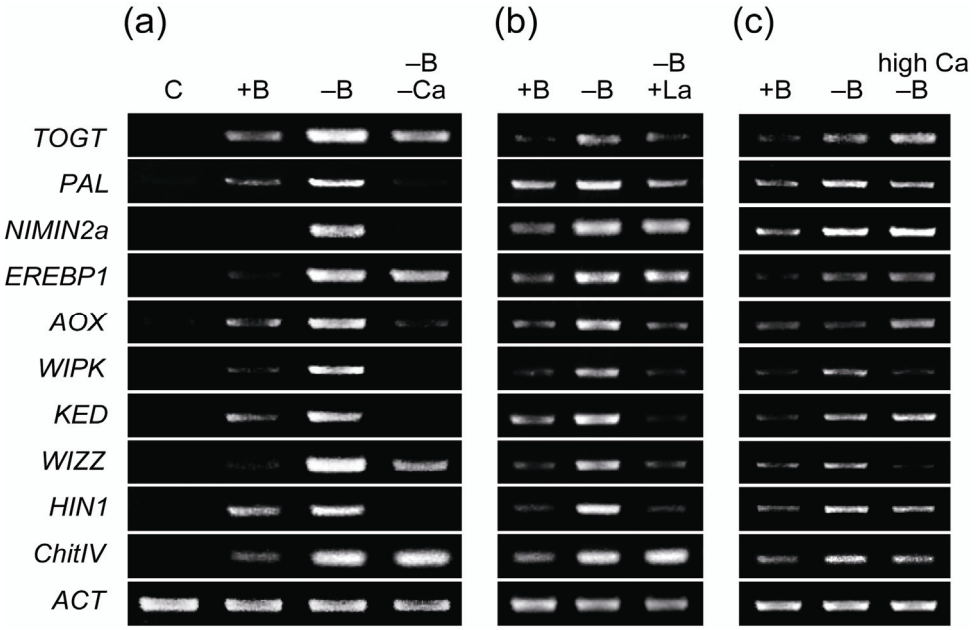

Fig. 3.1 Boron deprivation-induced expression of stress-responsive genes of tobacco. Cells were washed with and resuspended in (a) standard (+B), B-free (–B) or B- and Ca-free (–B–Ca) culture medium, or (b) standard (+B), B-free (–B) culture medium or B-free culture medium supplemented with 1.5 mM La^{3+} (–B+La). (c) Cells were treated as in (a) (+B and –B) or preincubated for 1 h in a medium containing 30 mM $CaCl_2$ prior to B deprivation (high Ca –B). Cells were harvested at 1 h after resuspension and analyzed for the expression of known stress-responsive genes by RT-PCR (see text). C: unwashed control cells. *ACT*: actin.

regulatory genes such as *WIPK*, *MEK1* (a MAPK kinase), *Nitf* (a bZIP transcription factor), and a 14-3-3 protein. Based on the result, the authors presumed that there could be a crosstalk among the systems for sensing P, K, and Fe nutrient status, or alternatively, that plants could have separate P, K, and Fe nutrient signal transduction pathways that share common components. Since *WIPK* was also up-regulated in B-deprived tobacco BY-2 cells in this study, I wondered whether the observed B deprivation responses might represent general stress responses which could be seen under other nutrient deficiencies as well. However, B deprivation-inducible *KED*, *WIZZ*, *AOX*, and *PAL* (Fig. 3.1) were not induced by 1-h P deprivation (data not shown), suggesting that at least a part of observed responses are characteristic of B deprivation. We also examined whether *Nitf*, which exhibits the strongest and

Table 3.2 SA content of the cells with +B or –B treatment

Time (h)	Salicylic acid (ng g FW^{-1})	
	+B	–B
0.5	13.6 ± 2.6	16.3 ± 1.8
1	9.7 ± 1.8	8.9 ± 1.4

Value represents mean ± SD (n=3).

most rapid up-regulation upon P, K, or Fe withholding in tomato plants (Wang et al. 2002), responded similarly upon B deprivation. However, in tobacco BY-2 cells, deprivation of neither B nor P induced the up-regulation of *TGA1a*, the tobacco ortholog of *Nitf* (data not shown).

TOGT, *PAL*, *NIMIN2a*, *EREBP1*, and *AOX* are salicylic acid (SA)-inducible genes (Horvath and Chua 1996, Horvath et al. 1998, Ji and Ding 2001, Pellegrini et al. 1994). Induction of these genes upon B deprivation prompted me to examine if SA was involved in early response of tobacco cells to B deprivation. Unwashed control cells contained 8.3 ± 0.9 ng SA per gram fresh weight. SA content of 0.5-h –B cells was slightly higher than this value, but was not significantly different from that of 0.5-h +B cells (Table 3.2). Thus I could not ascribe the observed up-regulation of SA-responsive genes to a short-term SA accumulation. Induction of those genes may not be exclusive to SA, or there may be crosstalk between signaling pathways for SA and –B responses.

I found that external calcium (Ca^{2+}) concentration significantly affected the –B-responsive gene expression. Withholding Ca^{2+} from the medium inhibited the up-regulation of all genes except *EREBP1* and *ChitIV* (Fig. 3.1a). Adding lanthanum (La^{3+}) to the medium also suppressed the change (Fig. 3.1b). These results suggest that Ca^{2+} is involved in –B response. Aside from Ca^{2+} withholding, a higher dose of Ca^{2+} also affected the –B-responsive gene expression. Preincubating cells for 1 h in a medium containing 30 mM Ca^{2+}, which is 10 times higher than that contained in standard culture medium, abolished –B response of *WIPK* and *WIZZ* (Fig. 3.1c), which are known to be wound-inducible. Expression of SA-inducible genes (*TOGT*, *PAL*, *NIMIN2a*, *EREBP1*, or *AOX*) was not affected significantly (Fig. 3.1c). Besides B, Ca^{2+} also

cross-links pectic polysaccharides via the interaction with unesterified polygalacutronic acid regions (Jarvis 1984). Since the strength of Ca^{2+}-pectate gel increases with increasing Ca^{2+} concentration, higher amounts of Ca^{2+} could produce more stabilized pectic network. The treatment attenuated –B-induced expression of wound responsive genes (*WIPK* and *WIZZ*, Fig. 3.1c), suggesting that the disturbed pectic network structure triggers –B stress signaling.

To obtain further evidence for the Ca^{2+} involvement in –B stress signaling, I examined Ca^{2+} influx into B-deprived cells using aequorin-expressing tobacco BY-2 cells (Takahashi et al. 1997). If B deprivation lets Ca^{2+} channels open, –B cells would uptake more Ca^{2+}, and therefore emit stronger aequorin luminescence than +B cells. The standard culture medium for tobacco BY-2 cells contains 3 mM $CaCl_2$. For this experiment, cells containing reconstituted aequorin were washed with and resuspended in a medium containing minimal concentration of $CaCl_2$ (20 μM) with or without B. This was to maintain the integrity of cell wall and membrane, but not to allow Ca^{2+} influx during the treatment. External Ca^{2+} concentration was then raised to 3 mM to trigger Ca^{2+} influx through the opened channels. As shown in Fig. 3.2a, –B cells emitted a luminescence twice as strong as that emitted by +B cells. No change in luminescence was observed when water instead of $CaCl_2$ was added to the suspension (data not shown). Luminescence emission from –B cells was completely suppressed by 1.5 mM of either La^{3+} (Fig. 3.2b) or Gd^{3+} (data not shown). These results collectively suggest that the observed luminescence represents a Ca^{2+} influx through channels. Since +B cells also emitted significant luminescence (Fig. 3.2a), the luminescence from –B cells could be due in part to a mechanical stress-induced Ca^{2+} influx. Nonetheless, –B cells emitted reproducibly more intense luminescence than +B cells (Fig. 3.2a), suggesting that the difference between treatments represents the effect of B deprivation. Taken together, we conclude that B deprivation induces an opening of a certain type of Ca^{2+} channels. The change occurred within minutes after disappearance of B from the external medium, since in this experiment Ca^{2+} uptake was measured as early as seven minutes after the onset of washing procedure.

As shown in Fig. 3.2b, diphenyleneiodonium (DPI), a plasma membrane NAD(P)H oxidase inhibitor, suppressed 80% of luminescence emission from –B cells. This result suggests that reactive oxygen species (ROS) produced by NAD(P)H oxidase are necessary to activate–B-induced Ca^{2+} influx. Mitogen-activated protein kinase (MAPK) seems to work

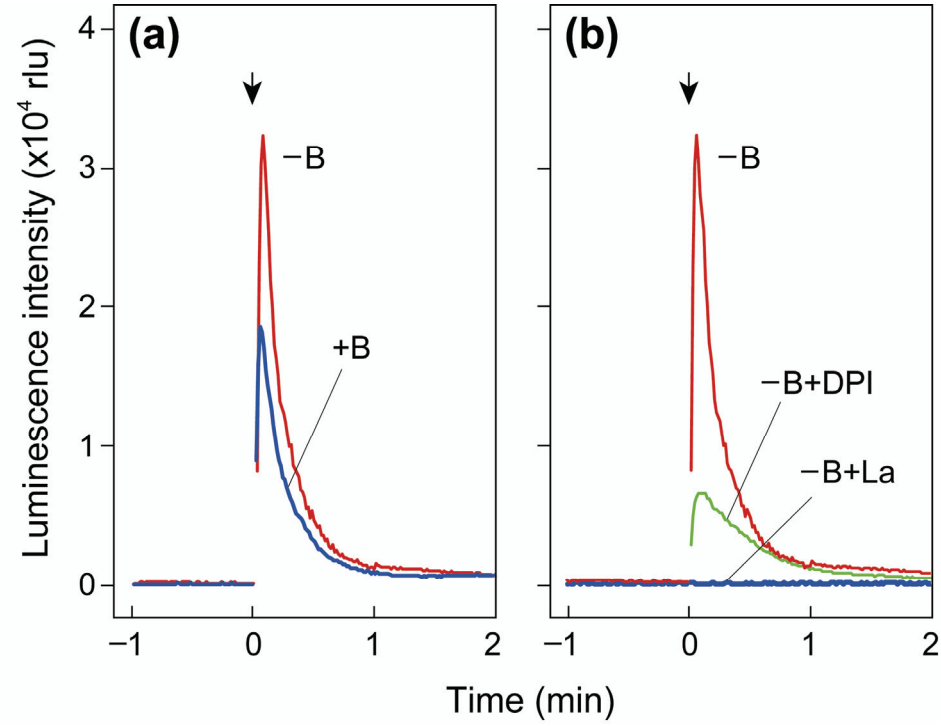

Fig. 3.2 Aequorin luminescence from B-deprived cells. (a) Typical traces of luminescence emitted from +B and –B cells. Cells were washed with and resuspended in a low Ca^{2+} medium with or without B. Ca^{2+} influx was triggered by raising external Ca^{2+} at the time indicated by arrows. (b) Effect of La^{3+} and DPI on the luminescence emission –B cells. Cells were treated as in (a) except that B-free medium was supplemented with 1.5 mM $LaCl_3$ or 50 μM DPI. Shown are the representative traces of 10 experiments. rlu, relative light units.

downstream of Ca^{2+} influx, since B derivation induced *WIPK* expression in a Ca^{2+}-dependent manner (Fig. 3.1a). Thus I identified Ca^{2+}, ROS and MAPK as the possible components of –B stress signaling pathway. To my knowledge, this is the first report to show that Ca^{2+} can act in plant responses to nutrient deprivation.

In Chapter 1, I have discussed about possible involvement of cell wall-membrane interaction in –B stress signaling. The notion was supported by the fact that the higher amounts of Ca^{2+}, which could produce more stabilized pectic network, attenuated –B-induced expression of wound responsive genes (*WIPK* and *WIZZ*, Fig. 3.1c). To obtain further supporting evidence for the notion, I examined the effect of hyperosmosis on –B-responsive gene expression. From the –B-responsive genes included in Fig. 3.1, I have picked up the ones whose expression was not

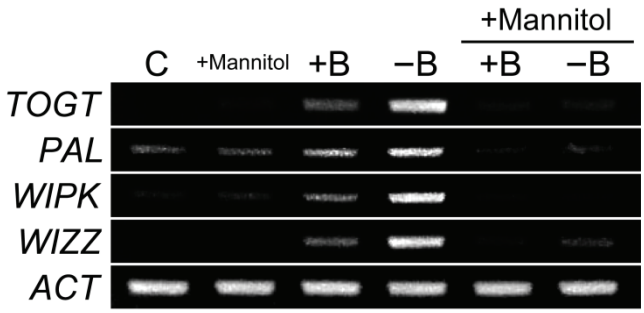

Fig. 3.3 Boron deprivation-induced expression of stress-responsive genes of tobacco. Cells were washed with and resuspended in standard (+B), B-free (–B), standard or B-free culture medium supplemented with 0.4 M mannitol (+B+Mannitol and –B+Mannitol). C: unwashed control cells. +Mannitol: unwashed and 0.4 M mannitol control cells. *ACT*: actin.

up-regulated with 0.4 M mannitol alone. The picked up genes include *TOGT*, *PAL*, *WIPK*, and *WIZZ*. As shown in Fig. 3.3, –B-induced expression of these four genes were strongly suppressed in the presence of 0.4 M mannitol. This result is consistent with the notion that membrane stretch may trigger –B responses.

It remains to be confirmed whether the B-RG-II complex is decomposed immediately after B deprivation. B-RG-II complex are highly stable in vitro (Kobayashi et al. 1999) and it is unclear at this time whether B-RG-II complex in cell wall decomposes immediately after B deprivation. However, it is possible that the B-RG-II bonding *in vivo* is less stable than *in vitro*, or that a failure in cross-linking newly secreted polysaccharides is critical. Whatever the case, the mechanical strength of cell wall could be affected immediately upon B deprivation, as shown in squash root cell (Findeklee et al. 1997).

As plant cell walls enclose protoplasm and counteract its osmotic pressure, decrease in tensile strength of the cell wall could lead to an expansion of the protoplasm. The change would impose stretch-stress on plasma membranes to trigger the cell's signaling cascades. Consistent with this speculation, I found that a high dose of Ca^{2+}, which may stabilize the pectic network structure, and hyperosmosis, which may inhibit the membrane stretch, abolished –B response of some genes (Fig. 3.1c). Hence I propose that plasma membrane mechanosensitive Ca^{2+} channel(s) are involved in B deprivation response of tobacco BY-2 cells. In yeast, similar

mechanism involving stretch-activated Ca^{2+} channel and MAPK senses and maintains cell wall integrity (Levin 2005). In this study, –B-induced Ca^{2+} influx was suppressed by DPI, a plasma membrane NAD(P)H oxidase inhibitor (Fig. 3.2b). Several types of Ca^{2+}-permeable channels are activated by ROS, while mechanosensitive Ca^{2+} channels are not. Therefore a plausible mechanism is that a mechanosensitive Ca^{2+} channel mediates an initial Ca^{2+} uptake, which in turn activates ROS production by NAD(P)H oxidase and secondary Ca^{2+} influx through separate ROS-responsive channels. RNAi suppression of mechanosensitive channels such as MCA1 (Nakagawa et al. 2007) would be necessary to examine this hypothesis.

Conclusion

Boron (B) cross-links pectic polysaccharides at the rhamnogalacturonan II (RG-II) regions thereby contributes to building the cell wall structure. However, it remains unknown how B deficiency triggers various metabolic disorders and brings about cell death. To understand this mechanism, I have analyzed the response of cultured tobacco BY-2 cells to B deprivation.

I revealed that oxidative damage is the direct cause of cell death induced by B deficiency. Although the dead cells exhibited a characteristic morphology with shrunken cytoplasm which is often seen in cells undergoing PCD, the mode of cell death was necrosis.

Transcriptome analysis revealed that the genes for primary metabolism and/or damage repair system were induced upon B deprivation, while those for the modification of cell wall structure were not.

Tobacco cells could sense B depletion immediately after the treatment, probably through a physical change in cell wall structure. Ca^{2+} influx was necessary to trigger the early responses.

Based on these results, I have proposed a scheme for the response of plant cells to B deficiency. Insufficient cross-linking of pectic polysaccharides with B makes cell wall weaker and less resistant to turgor pressure. The change leads to an expansion of cytoplasm and the activation of Ca^{2+} influx through stretch-activated Ca^{2+} channels in plasma membrane. The entered Ca^{2+} triggers –B responses including gene expression and also production of ROS from NADPH oxidase. The cells attempt to survive the oxidative stress. However, since cells can not maintain cell wall integrity without B, the Ca^{2+} influx and ROS production persist and lead to oxidative damage and cell death eventually.

Acknowledgements

The present thesis is based on the studies carried out at Plant Nutrition Laboratory, Graduate School of Agriculture, Kyoto University.

I am deeply grateful to Professor Toru Matoh for his guidance and encouragement during this investigation.

I am deeply grateful to Professor Emeritus Jiro Sekiya for his guidance and encouragement during this investigation.

I would like to express my gratitude to Dr. Masaru Kobayashi, Associate Professor of Plant Nutrition Laboratory, for his continuous guidance and discussion throughout this study.

I owe a very important debt to Dr. Kumiko Ochiai, Assistant Professor of Plant Nutrition Laboratory, for her advice and help for this study.

I owe a very important debt to the members proceeded earlier study on B in Plant Nutrition Laboratory. I wish to express my thanks to all the members in Plant Nutrition Laboratory, especially Dr. Yoshihiro Nakano, Dr. Akira Matsuda, Mr. Hirofumi Otoshi, Mr. Buichiro Shakudo, Mr. Shintaro Baba, Ms. Tomoko Inoue, Mr. Shin'ichi Uemura, Mr. Satoshi Fujita and Mr. Yuma Takagi, for their encouragement, discussion and advice.

Finally I would also like to express my gratitude to my parents for their moral support and warm encouragements.

Taichi Koshiba

References

Aebi, H. (1984) Catalase in vitro. *Methods Enzymol.* **105**: 121-126.

Ahn, J.W., Verma, R., Kim, M., Lee, J.Y., Kim, Y.K., Bang, J.W., Reiter, W.D. and Pai, H.S. (2006) Depletion of UDP-$_D$-apiose/UDP-$_D$-xylose synthases results in rhamnogalacturonan-II deficiency, cell wall thickening, and cell death in higher plants. *J. Biol. Chem.* **281**: 13708-13716.

Altschul, S.F., Gish, W., Miller, W., Myers, E.W. and Lipman, D.J. (1990) Basic local alignment search tool. *J. Mol. Biol.* **215**: 403-410.

Asada, K. (1984) Chloroplasts: formation of active oxygen and its scavenging. *Methods Enzymol.* **105**: 422-429.

Bassil. E., Hu. H. and Brown, P.H. (2004) Use of phenylboronic acids to investigate boron function in plants. Possible role of boron in transvacuolar cytoplasmic strands and cell-to-wall adhesion. *Plant Physiol.* **136**: 3383-3395.

Bradford, M.M. (1976) A rapid and sensitive method for the quantitation of microgram quantities of protein utilizing the principle of protein-dye binding. *Anal. Biochem.* **72**: 248-254.

Bennett, A., Rowe, R.I., Soch, N. and Eckhert, C.D. (1999) Boron stimulates yeast (*Saccharomyces cerevisiae*) growth. *J. Nutr.* **129**: 2236-2238.

Blaser-Grill, J., Knoppik, D., Amberger, A. and Goldbach, H. (1989) Influence of boron on the membrane potential in *Elodea densa* and *Helianthus annuus* roots and H^+ extrusion of suspension cultured *Daucus carota* cells. *Plant Physiol.* **90**: 280-284.

Blevins, D.G. and Lukaszewski, K.M. (1998) Boron in plant structure and function. *Annu. Rev. Plant Physiol. Plant Mol. Biol.* **49**: 481-500.

Brown, P.H., Bellaloui, N., Wimmer, M.A., Bassil, E.S., Ruiz, J., Hu, H., Pfeffer, H., Dannel, F. and Römheld, V. (2002). Boron in plant biology. *Plant Biol.* **4**: 205-223.

Cakmak, I., Kurz, H. and Marschner, H. (1995) Short-term effects of boron, germanium and high light intensity on membrane permeability in boron deficient leaves of sunflower. *Physiol. Plant.* **95**: 11-18.

Cakmak, I. and Römheld, V. (1997) Boron deficiency-induced impairments of cellular functions in plants. *Plant Soil* **193**: 71-83.

Camacho-Cristóbal, J.J., Anzelotti, D. and González-Fontes, A. (2002) Changes in phenolic metabolism of tobacco plants during short-term boron deficiency. *Plant Physiol. Biochem.* **40**: 997-1002.

Camacho-Cristóbal, J.J. and González-Fontes, A. (1999) Boron deficiency causes a drastic decrease in nitrate content and nitrate reductase activity, and increases the content of carbohydrates in leaves from tobacco plants. *Planta* **209**: 528-536.

Camacho-Cristóbal, J.J. and González-Fontes, A. (2007) Boron deficiency decreases plasmalemma H^+-ATPase expression and nitrate uptake, and promotes ammonium assimilation into asparagine in tobacco roots. *Planta* **226**: 443-451.

Camacho-Cristóbal, J.J., Herrera-Rodríguez, M.B., Beato, V.M., Rexach, J., Navarro-Gochicoa, M.T., Maldonado, J.M. and González-Fontes, A. (2008) The expression of several cell wall-related genes in *Arabidopsis* roots is down-regulated under boron deficiency. *Env. Exp. Bot.* **63**: 351-358.

Camacho-Cristóbal, J.J., Lunar, L., Lafont, F., Baumert, A., González-Fontes, A. (2004) Boron deficiency causes accumulation of chlorogenic acid and caffeoyl polyamine conjugates in tobacco leaves. *J. Plant Physiol.* **161**: 879-881.

Camacho-Cristóbal, J.J., Maldonado, J.M. and González-Fontes, A. (2005) Boron deficiency increases putrescine levels in tobacco plants. *J. Plant Physiol.* **162**: 921-928.

Casolo, V., Petrussa, E., Krajnáková, J., Macrì, F. and Vianello, A. (2005) Involvement of the mitochondrial K^+ATP channel in H_2O_2- or NO-induced programmed death of soybean suspension cell cultures. *J. Exp. Bot.* **56**: 997-1006.

Clarke, A., Desikan, R., Hurst, R.D., Hancock, J.T. and Neill, S.J. (2000) NO way back: nitric oxide and programmed cell death in Arabidopsis thaliana suspension cultures. *Plant J.* **24**: 667-677.

Cosgrove, D.J. (1999) Enzymes and other agents that enhance cell wall extensibility. *Annu. Rev. Plant Physiol. Plant Mol. Biol.* **50**: 391-417.

Demura, T., Tashiro, G., Horiguchi, G. Kishimoto, N., Kubo, M., Matsuoka, N., Minami, A., Nagata-Hiwatashi, M., Nakamura, K., Okamura, Y., Sassa, N., Suzuki, S., Yazaki, J., Kikuchi, S. and Fukuda, H. (2002) Visualization by comprehensive microarray analysis of gene expression programs during transdifferentiation of mesophyll cells into xylem cells. *Proc. Natl. Acad. Sci. U.S.A.* **99**: 15794-15799.

de Pinto, M.C., Paradiso, A., Leonetti, P. and De Gara, L. (2006) Hydrogen peroxide, nitric oxide and cytosolic ascorbate peroxidase at the crossroad between defence and cell death. *Plant J.* **48**: 784-795.

de Pinto, M.C., Tommasi, F. and De Gara, L. (2002) Changes in the antioxidant systems as part of the signaling pathway responsible for the programmed cell death activated by nitric oxide and reactive oxygen species in tobacco Bright-Yellow 2 cells. *Plant Physiol.* **130**: 698-708.

Duval, I., Brochu, V., Simard, M., Beaulieu, C. and Beaudoin, N. (2005) Thaxtomin A induces programmed cell death in *Arabidopsis thaliana* suspension-cultured cells. *Planta* **222**: 820-831.

Eckhert, C.D. (1998) Boron stimulates embryonic trout growth. *J. Nutr.* **128**: 2488-2493.

Eckhert, C.D. and Rowe, R.I. (1999) Embryonic dysplasia and adult retinal dystrophy in boron-deficient zebrafish. *J. Trace Elem. Exp. Med.* **12**: 213-219.

Ellis, C., Karafyllidis, I., Wasternack, C. and Turner, J.G. (2002) The Arabidopsis mutant *cev1* links cell wall signaling to jasmonate and ethylene responses. *Plant Cell* **14**: 1557-1566.

Ferrol, N. and Donaire, J.P. (1992) Effect of boron on plasma membrane proton extrusion and redox activity in sunflower cells. *Plant Sci.* **86**: 41-47.

Fort, D.J., Propst, T.L., Stover, E.L., Strong, P.L. and Murray, F.J. (1998) Adverse reproductive and developmental effects in *Xenopus* from insufficient boron. *Biol. Trace Elem. Res.* **66**: 237-259

Frantzen, F., Grimsrud, K., Heggli, D.E. and Sundrehagen, E. (1995) Protein-boronic acid conjugates and their binding to low-molecular-mass *cis*-diols and glycated hemoglobin. *J Chromatogr. B* **670**: 37-45.

Friedman, S., Pace, B. and Pizer, R. (1974) Complexation of phenylboronic acid with lactic acid. Stability constant and reaction kinetics. *J. Am. Chem. Soc.* **96**: 5381-5384.

Findeklee, P. and Goldbach, H.E. (1996) Rapid effects of boron deficiency on cell wall elasticity modulus in *Cucurbita pepo* roots. *Bot. Acta* **109**: 463-465.

Findeklee, P., Wimmer, M. and Goldbach, H.E. (1997) Early effects of boron deficiency on physical cell wall parameters, hydraulic conductivity and plasmalemma-bound reductase activities in young *C. pepo* and *V. faba* roots. *In*: Boron in Soils and Plants. Bell RW, Rerkasem B, eds. Dordrecht, The Netherlands: Kluwer Academic Publishers. 221-227.

Fleischer, A., O'Neill, M.A. and Ehwald, R. (1999). The pore size of non-graminaceous plant cell walls is rapidly decreased by borate ester cross-linking of the pectic polysaccharide rhamnogalacturonan II. *Plant Physiol.* **121**: 829-838.

Foyer, C.H., Lelandais, M. and Kunert, K.J. (1994) Photooxidative stress in plants. *Physiol. Plant.* **92**: 696-717.

Gális, I., Simek, P., Narisawa, T., Sasaki, M., Horiguchi, T., Fukuda, H. and Matsuoka, K. (2006) A novel R2R3 MYB transcription factor NtMYBJS1 is a methyl jasmonate-dependent regulator of phenylpropanoid-conjugate biosynthesis in tobacco. *Plant J.* **46**: 573-592.

Goldbach, H.E. (1997) A critical review on current hypotheses concerning the role of boron in higher plants: suggestions for further research and methodological requirements. *J. Trace and Microprobe Tech.* **15**: 51-91.

Goldbach, H.E., Yu, Q., Wingender, R., Schulz, M., Wimmer, M., Findeklee, P. and Baluška, F. (2001) Rapid response reactions of roots to boron deprivation. *J. Plant Nutr. Soil. Sci.* **164**: 173-181.

Goldbach, H.E. and Wimmer, M. (2007) Boron in plants and animals: Is there a role beyond cell-wall structure? *J. Plant Nutr. Soil Sci.* **170**: 39-48.

Gopalan, S., Wei, W. and He, S.Y. (1996) *hrp* gene-dependent induction of *hin1*: a plant gene activated rapidly by both harpins and the *avrPto* gene-mediated signal. *Plant J.* **10**: 591-600.

Hara, K., Yagi, M., Koizumi, N., Kusano, T. and Sano, H. (2000a) Screening of wound-responsive genes identifies an immediate-early expressed gene encoding a highly charged protein in mechanically wounded tobacco plants. *Plant Cell Physiol.* **41**: 684-691.

Hara, K., Yagi, M., Kusano, T. and Sano, H. (2000b) Rapid systemic accumulation of transcripts encoding a tobacco WRKY transcription factor upon wounding. *Mol. Gen. Genet.* **263**: 30-37.

Hirsch, A.M. and Torrey, J.G (1980) Ultrastructural changes in sunflower root cells in relation to boron deficiency and added auxin. *Can. J. Bot.* **58**: 856-866.

Hoson, T. (1998) Apoplast as the site of response to environmental signals. *J. Plant Res.* **111**: 167-177.

Horvath, D.M. and Chua, N.H. (1996) Identification of an immediate-early salicylic acid-inducible tobacco gene and characterization of induction by other compounds. *Plant Mol. Biol.* **31**: 1061-1072.

Horvath, D.M., Huang, D.J. and Chua, N.H. (1998) Four classes of salicylate-induced tobacco genes. *Mol. Plant Microbe Interact.* **11**: 895-905.

Hu, H., Brown, P.H. and Labavitch, J.M. (1996) Species variability in boron requirement is correlated with cell wall pectin. *J. Exp. Bot.* **47**: 227-232.

Hu, H. and Brown, P.H. (1994) Localization of boron in cell walls of squash and tobacco and its association with pectin. *Plant Physiol.* **105**: 681-689.

Ishii, T. and Matsunaga, T. (1996) Isolation and characterization of a boron-rhamnogalacturonan-II complex from cell walls of sugar beet pulp. *Carbohydr. Res.* **284**: 1-9.

Iwai, H., Masaoka, N., Ishii, T. and Satoh, S. (2002) A pectin glucuronyltransferase gene is essential for intercellular attachment in the plant meristem. *Proc. Natl. Acad. Sci. U.S.A.* **99**: 16319-16324.

Jagendorf, A.T. and Takabe, T. (2001) Inducers of glycinebetaine synthesis in barley. *Plant Physiol.* **127**: 1827-1835.

Jarvis, M.C. (1984) Structure and properties of pectin gels in plant cell walls. *Plant Cell Environ.* **7**: 153-164.

Ji, L.H. and Ding, S.W. (2001) The suppressor of transgene RNA silencing encoded by Cucumber mosaic virus interferes with salicylic acid-mediated virus resistance. *Mol. Plant Microbe Interact.* **14**: 715-724.

Kaneko, S., Ishii, T. and Matsunaga, T. (1997) A boron-rhamnogalacturonan-II complex from bamboo shoot cell walls. *Phytochemistry* **44**: 243-248.

Klapheck, S., Fliegner, W. and Zimmer, I. (1994) Hydroxymethyl-phytochelatins [$(\gamma$-glutamylcysteine$)_n$-serine] are metal-induced peptides of the Poaceae. *Plant Physiol.* **104**: 1325-1332.

Kobayashi, M., Matoh, T. and Azuma, J. (1996) Two chains of rhamnogalacturonan II are cross-linked by borate-diol ester bonds in higher plants cell walls. *Plant Physiol.* **110**: 1017-1020.

Kobayashi, M., Ohno, K. and Matoh, T. (1997) Boron nutrition of tobacco BY-2 cells. II. Characterization of the boron–polysaccharide complex. *Plant Cell Physiol.* **38**: 676-683.

Kobayashi, M., Nakagawa, H., Asaka, T. and Matoh, T. (1999) Borate-rhamnogalacturonan II bonding reinforced by Ca^{2+} retains pectic polysaccharides in higher-plant cell walls. *Plant Physiol.* **119**: 199-204.

Kouchi, H. and Kumazawa, K. (1976) Anatomical responces of root tips to boron deficiency. III: Effect of boron deficiency on sub-cellular structure of root tips, particularly on morphology of cell wall and its related organelles. *Soil Sci. Plant Nutr.* **22**: 53-71.

Kroemer, G., Dallaporta, B. and Resche-Rigon, M. (1998) The mitochondrial death/life regulation in apoptosis and necrosis. *Annu. Rev. Physiol.* **60**: 619-642.

Lanoue, L., Trollinger, D.R., Strong, P.L., and Keen, C.L. (2000) Functional impairments in preimplantation mouse embryos following boron deficiency. *FASEB J.* **14A**: 539.

Lecourieux, D., Ranjeva, R. and Pugin, A. (2006) Calcium in plant defence-signalling pathways. *New Phytol.* **171**: 249-269.

Lee, S.G. and Aronoff, S. (1966) Investigations on the role of boron in plants. III. Anatomical observations. *Plant Physiol.* **41**: 1570-1577.

Lemarchand, D., Gaillardet, J., Lewin, E. and Allègre, C.J. (2000) The influence of rivers on marine boron isotopes and implications for reconstructing past ocean pH. *Nature* **408**: 951-954.

Levin, D.E. (2005) Cell wall integrity signaling in *Saccharomyces cerevisiae*. *Microbiol. Mol. Biol. Rev.* **69**: 262-291.

Lewis, D.H. (1980) Boron, lignifications and the origin of vascular plants – a unified hypothesis. *New Phytol.* **84**: 209-229.

Loomis, W.D. and Durst, R.W. (1992) Chemistry and biology of boron. *Biofactors* **3**: 229-239.

Lukaszewski, K.M. and Blevins, D.G. (1996) Root growth inhibition in boron-deficient or aluminum-stressed squash may be a result of impaired ascorbate metabolism. *Plant Physiol.* **112**: 1135-1140.

Loomis, W.D. and Durst, R.W. (1992) Chemistry and biology of boron. *BioFactors* **3**: 229-239.

Ma, J.F., Shen, R., Nagao, S., Tanimoto, E. (2004) Aluminum targets elongating cells by reducing cell wall extensibility in wheat roots. *Plant Cell Physiol.* **45**: 583-589.

Marschner, H. (1995) *Mineral Nutrition of Higher Plants.* 2nd ed. Academic Press, San Diego. pp. 379-396.

Matsuoka, K., Demura, T., Galis, I., Horiguchi, T., Sasaki, M., Tashiro, G. and Fukuda, H. (2004) A comprehensive gene expression analysis toward the understanding of growth and differentiation of tobacco BY-2 cells. *Plant Cell Physiol.* **45**: 1280-1289.

Matoh, T., Ishigaki, K., Mizutani, M., Matsunaga, W. and Takabe, K. (1992) Boron nutrition of cultured tobacco BY-2 cells. I. Requirement for and intracellular localization of boron and selection of cells that tolerate low levels of boron. *Plant Cell Physiol.* **33**: 1135-1141.

Matoh, T., Ishigaki, K., Ohno, K. and Azuma, J. (1993) Isolation and characterization of a boron-polysaccharide complex from radish roots. *Plant Cell Physiol.* **34**: 639-642.

Matoh, T., Kawaguchi, S. and Kobayashi, M. (1996) Ubiquity of a borate-rhamnogalacturonan II complex in the cell walls of higher plants. *Plant Cell Physiol.* **37**: 636-640.

Matoh, T., Takasaki, M., Kobayashi, M. and Takabe, K. (2000) Boron Nutrition of Cultured Tobacco BY-2 Cells. III. Characterization of the Boron-Rhamnogalacturonan II Complex in Cells Acclimated to Low Levels of Boron. *Plant Cell Physiol.* **41**: 363-366.

Maxwell, D.P., Wang, Y. and McIntosh, L. (1999) The alternative oxidase lowers mitochondrial reactive oxygen production in plant cells. *Proc. Natl. Acad. Sci. U.S.A.* **96**: 8271-8276.

Murray, M.G. and Thompson, W.F. (1980) Rapid isolation of high molecular weight plant DNA. *Nucleic Acids Res.* **8**:4321-4325.

Nagata, T., Okada, K., Takebe, I. and Matsui, C. (1981) Delivery of tobacco mosaic virus RNA into plant protoplasts mediated by reverse-phase evaporation vesicles (liposomes). *Mol. Gen. Genet.* **184**: 161-165.

Nakagawa, Y., Katagiri, T., Shinozaki, K., Qi, Z., Tatsumi, H., Furuichi, T., Kishigami, A., Sokabe, M., Kojima, I., Sato, S., Kato, T., Tabata, S., Iida, K., Terashima, A., Nakano, M., Ikeda, M., Yamanaka, T. and Iida, H. (2007) *Arabidopsis* plasma membrane protein crucial for Ca^{2+} influx and touch sensing in roots. *Proc. Natl. Acad. Sci. U.S.A.* **104**: 3639-3644.

Nielsen, F.H. (2000) The emergence of boron as nutritionally important throughout the life cycle. *Nutrition* **16**: 512-514.

O'Neill, M.A., Eberhard, S., Albersheim, P. and Darvill, A.G. (2001) Requirement of borate cross-linking of cell wall rhamnogalacturonan II for *Arabidopsis* growth. *Science* **294**: 846-849.

O'Neill, M.A., Ishii, T., Albersheim, P. and Darvill, A.G. (2004) Rhamnogalacturonan II: structure and function of a borate cross-linked cell wall pectic polysaccharide. *Annu. Rev. Plant Biol.* **55**: 109-139.

Parr, A.J. and Loughman, B.C. (1983) Boron and membrane function in plants. *In*: Metals and Micronutrients. Uptake and Utilization by Plants. Robb DA, Pierpoint WS, eds. New York: Academic Press. 87-107.

Pellegrini, L., Rohfritsch, O., Fritig, B. and Legrand, M. (1994) Phenylalanine ammonia-lyase in tobacco. Molecular cloning and gene expression during the hypersensitive reaction to tobacco mosaic virus and the response to a fungal elicitor. *Plant Physiol.* **106**: 877-886.

Pellerin, P., Doco, T., Vidal, S., Williams, P., Brillouet, J.M. and O'Neill, M.A. (1996) Structural characterization of red wine rhamnogalacturonan II. *Carbohydr. Res.* **290**: 183-197.

Power, P.P. and Woods, W.G. (1997) The chemistry of boron and its speciation in plants. *Plant Soil* **193**: 1-13.

Purvis, A.C. (1997) Role of the alternative oxidase in limiting superoxide production by plant mitochondria. *Physiol. Plant.* **100**: 165-170.

Raven, J.A. (1980) Short- and long-distance transport of boric acid in plants. *New Phytol.* **84**: 231-249.

Rowe, R.I. and Eckhert, C.D. (1999) Boron is required for zebrafish embryogenesis. *J. Exp. Biol.* **202**: 1649-1654.

Rowe, R.I., Bouzan, C., Nabili, S. and Eckhert, C.D. (1998) The response of trout and zebrafish embryos to low and high boron concentrations is U-shaped. *Biol. Trace Elem. Res.* **66**: 262-270.

Ryden, P., Sugimoto-Shirasu, K., Smith, A.C., Findlay, K., Reiter, W.D. and McCann, M.C. (2003) Tensile properties of *Arabidopsis* cell walls depend on both a xyloglucan cross-linked microfibrillar network and rhamnogalacturonan II-borate complexes. *Plant Physiol.* **132**: 1033-1040.

Scheffler, I.E. (1999) Mitochondria. Wiley-Liss, New York

Seo, S., Sano, H. and Ohashi, Y. (1999) Jasmonate-based wound signal transduction requires activation of WIPK, a tobacco mitogen-activated protein kinase. *Plant Cell* **11**: 289-298.

Shirzadegan, M., Christie, P. and Seemann, J.R. (1991) An efficient method for isolation of RNA from tissue cultured plant cells. *Nucleic Acids Res.* **19**: 6055.

Shorrocks, V. (1997) The occurrence and correction of boron deficiency. *Plant Soil* **193**: 121-148.

Shinya, T., Hanai, K., Galis, I., Suzuki, K., Matsuoka, K., Matsuoka, H. and Saito, M. (2007) Characterization of *NtChitIV*, a class IV chitinase induced by beta-1,3-, 1,6-glucan elicitor from *Alternaria alternata* 102: Antagonistic effect of salicylic acid and methyl jasmonate on the induction of *NtChitIV*. *Biochem. Biophys. Res. Commun.* **353**: 311-317.

Slater, F.T., Sawyer, B. and Sträuli, U. (1963) Studies on succinate-tetrazolium reductase systems. III. Points of coupling of four different tetrazolium salts. *Biochim. Biophys. Acta* **77**: 383-393.

Solomon, M., Belenghi, B., Delledonne, M., Menachem, E. and Levine, A. (1999) The involvement of cysteine proteases and protease inhibitor genes in the regulation of programmed cell death in plants. *Plant Cell* **11**: 431-443.

Sommer, A.L. and Lipman, C.B. (1926) evidence on the indispensable nature of zinc and boron for higher green plants. *Plant Physiol.* **1**: 231-249.

Spurr, A.R. (1957) The effect of boron on the cell wall structure in celery. *Amer. J. Bot.* **44**: 637-650.

Takahashi, K., Isobe, M., Knight, M.R., Trewavas, A.J. and Muto, S. (1997) Hypoosmotic shock induces increases in cytosolic Ca^{2+} in tobacco suspension-culture cells. *Plant Physiol.* **113**: 587-594.

Takano, J., Kyoko, M. and Fujiwara, T. (2008) Boron transport mechanisms: collaboration of channels and transporters. *Trends Plant Sci.* **13**: 451-457.

Tanaka, H. (1966) Response of *Lemna paucicostata* to boron as affected by light intensity. *Plant Soil* **25**: 425-434.

Tate, S.S. and Meister, A. (1978) Serine-borate complex as a transition-state inhibitor of gamma-glutamyl transpeptidase. *Proc. Natl. Acad. Sci. U.S.A.* **75**: 4806-4809.

Vacca, R.A., de Pinto, M.C., Valenti, D., Passarella, S., Marra, E. and De Gara, L. (2004) Production of reactive oxygen species, alteration of cytosolic ascorbate peroxidase, and impairment of mitochondrial metabolism are early events in heat shock-induced programmed cell death in tobacco Bright-Yellow 2 cells. *Plant Physiol.* **134**: 1100-1112.

Wang, Y.H., Garvin, D.F. and Kochian, L.V. (2002) Rapid induction of regulatory and transporter genes in response to phosphorus, potassium, and iron deficiencies in tomato roots. Evidence for cross talk and root/rhizosphere-mediated signals. *Plant Physiol.* **130**: 1361-1370.

Wang, Z.Y., Tang, Y.L., Zhang, F.S. and Wang, H. (1999). Effect of boron and low temperature on membrane integrity of cucumber leaves. *J. Plant Nutr.* **22**: 543-550.

Warington, K. (1923) The effect of boric acid and borax on the broad bean and certain other. *Ann. Bot.* **27**: 629-672

Weigel, R.R., Bauscher, C., Pfitzner, A.J. and Pfitzner, U.M. (2001) NIMIN-1, NIMIN-2 and NIMIN-3, members of a novel family of proteins from *Arabidopsis* that interact with NPR1/NIM1, a key regulator of systemic acquired resistance in plants. *Plant Mol. Biol.* **46**: 143-160.

Woods, W.G. (1996) Review of possible boron speciation relating to its essentiality. *J. Trace Elem. Exp. Med.* **9**: 153-163.

van Doorn, W.G. and Woltering, E.J. (2005) Many ways to exit? Cell death categories in plants. *Trends Plant Sci.* **10**: 117-122.

Yagi, K. (1984) Assay for blood plasma or serum. *Methods Enzymol.* **105**: 328-331.

Yamamoto, Y., Kobayashi, Y., Devi, S.R., Rikiishi, S. and Matsumoto, H. (2002) Aluminum toxicity is associated with mitochondrial dysfunction and the production of reactive oxygen species in plant cells. *Plant Physiol.* **128**: 63-72.

Yu, Q., Baluška, F., Jasper, F., Menzel, D. and Goldbach, H.E. (2003) Short-term boron deprivation enhances levels of cytoskeletal proteins in maize, but not zucchini, root apices. *Physiol. Plant.* **117**: 270-278.

Yu, Q., Wingender, R., Schulz, M., Baluška, F. and Goldbach, H.E. (2001) Short-term boron deprivation induces increased levels of cytoskeletal proteins in *Arabidopsis* roots. *Plant Biol.* **3**: 335-340.

Publications

Koshiba, T., Kobayashi, M. and Matoh, T. (2009) Boron nutrition of tobacco BY-2 cells. V. oxidative damage is the major cause of cell death induced by boron deprivation. *Plant Cell Physiol.* **50**: 26-36.

Koshiba, T., Kobayashi, M. and Matoh, T. (2009) Boron deficiency. How does the defect in cell wall damage the cells? *Plant Signal. Behav.* **4**: 557-558.

Koshiba, T., Kobayashi, M., Ishihara, A. and Matoh, T. (2010) Boron nutrition of cultured tobacco BY-2 cells. VI. Calcium is involved in early responses to boron deprivation. *Plant Cell Physiol. in press.*

Koshiba, T., Kobayashi, M., Matsuoka, K., Fujiwara, T. and Matoh, T. (2010) Boron nutrition of cultured tobacco BY-2 cells. VII. A comprehensive analysis of gene expression in cells deprived of boron. *in preparation.*

京都大学大学院
農学研究科応用生命科学専攻

学位請求論文講演要旨

Studies on Responses of Tobacco Cells to Boron Deprivation

(タバコ培養細胞のホウ素欠乏応答に関する研究)

小柴 太一

専門種目：植物栄養学
指導教員：間藤 徹 教授

平成 22 年 1 月

緒言

ホウ素（B）は植物の微量必須元素の一つである．植物細胞においてBの大部分は細胞壁に局在し，ペクチン質多糖のラムノガラクツロナンII（RG-II）領域とホウ酸ジエステルを形成する（Fig. 1）．このホウ酸架橋を破壊するとペクチン質多糖の溶出が起こることから，Bはペクチン質多糖をゲル化させ，細胞壁中に保持していると考えられる．すなわちBは細胞壁超分子構造の形成因子として機能している．

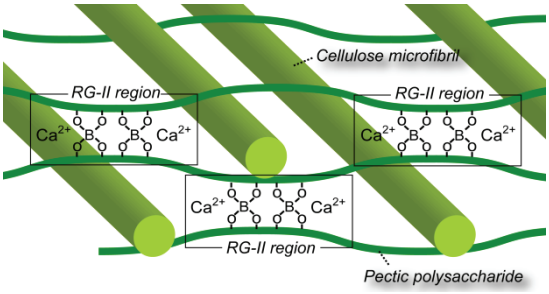

Fig. 1 植物の細胞壁構造の模式図．Bはペクチン質多糖のラムノガラクツロナンII（RG-II）領域とホウ酸ジエステルを形成し，ペクチン質多糖ネットワークを構築する．

一方，B欠乏による障害の発生機作は明らかでない．B欠乏では糖の輸送，細胞壁構造，炭水化物代謝，RNA代謝，呼吸，オーキシン代謝，フェノール代謝，膜輸送等の多様な過程に異常が発生し最終的に細胞は死に至る．Bの生理機能が細胞壁超分子構造の構築であるとすれば，これらB欠乏による障害や細胞死は細胞壁の構造異常が原因で発生するはずである．しかし細胞壁の構造異常と様々な代謝障害や細胞死の因果関係は不明である．そこで，タバコ培養細胞BY-2株（*Nicotiana tabacum* L. cv. Bright Yellow-2）を用いてB欠乏に対する応答を解析した．

1. ホウ素欠乏による細胞死の発生機作の解明

3日齢のタバコ培養細胞をB欠除（–B）処理すると処理後12時間から生存率の低下が明らかとなり48時間で生存率は約30%まで低下した（Fig. 2a）．死細胞は原形質凝集を起こし，細胞壁の変形も観察された（Fig. 2b）．

–Bの処理細胞をジヒドロエチジウムで染色すると，活性酸素種（ROS）の蓄積を示す赤色の蛍光が観察された．また，酸化障害の指標として過酸化脂質の蓄積を調べたところ，処理後36時間の細胞には対照（+B）細胞の約2倍量が蓄積していた．これらの結果は–B処理で酸化障害が起こることを示している．脂溶性抗酸化物質であるトコフェロールを培地に添加すると–B処理による細胞死は著しく抑制されたことから，酸化障害がB欠乏による細胞死の直接の原因であると結論した．

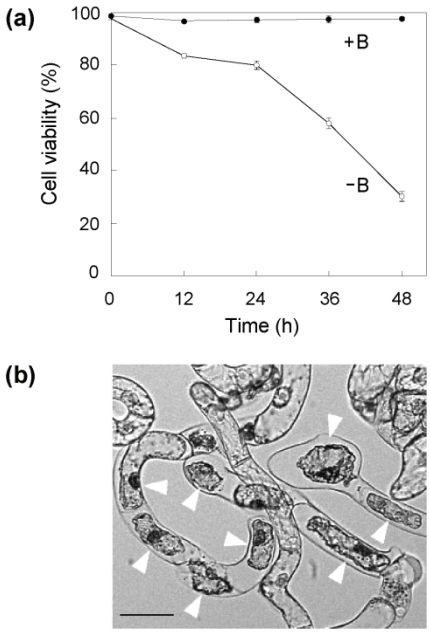

Fig. 2 B欠乏による細胞死．**(a)**細胞生存率の経時的変化．**(b)**原形質凝集を起こした死細胞

–B処理で死んだ細胞に見られた原形質凝集（Fig. 2b）は，プログラム細胞死（PCD）を起こした細胞でも観察される形態である．このことから，B欠乏による細胞死がPCDであるか，PCDの指標として核DNAの断片化，抗酸化

酵素の発現抑制・活性低下，抗酸化物質の減少，タンパク質合成阻害剤シクロヘキシミドによる細胞死抑制について検討したが結果はいずれも否定的であった．またすでに–B 処理による死細胞が顕在化している 18 時間の時点で 1 mg B l^{-1} となるようにホウ酸を再添加したところ，過酸化脂質含量は+B 処理区と同レベルまで減少し，その後の細胞死は抑制された．この結果は，B 欠乏による細胞死には PCD に見られる point of no return のような時点は存在しないことを示唆する．以上より，B 欠乏による細胞死は PCD ではなく，酸化障害のレベルが細胞の修復能力を超えることで起こるネクローシスであると結論した．

2. ホウ素欠乏に対する適応応答の解析

B 欠乏に際して細胞がどのような応答を示すか明らかにするため，約 16,000 の EST を含むタバコ cDNA マイクロアレイを用いて–B 細胞の遺伝子発現変化を解析した．解析には–B 処理後 1, 3, 6, 12, 36 時間の細胞を用い，いずれかの時点で–B 処理区の発現量が+B 処理区の 2 倍以上または 1/2 以下に変化した遺伝子を抽出した．2 回の反復で再現性が得られることを条件にフィルタリングし，最終的に 118 個の遺伝子を B 欠乏応答性遺伝子として同定した（Fig. 3）．これら遺伝子の大部分は，–B 処理 1 時間後に発現が抑制された後，3〜6 時間で一過的に発現量が上昇し，12 時間以降は+B との差が認められなくなった．

BLASTX 検索により機能を推定できた遺伝子は 61 個で，多くは転写，タンパク質合成，代謝，修復に関わる遺伝子であった（Fig. 3）．ストレス応答性遺伝子は他種ストレスでも誘導される感染や ROS の消去に関わるもので，酸化ストレスに対する適応応答と推測した．また，細胞壁構造の強化等，B の機能を代替すると期待されるようなタンパク質の遺伝子は見つからなかった．

以上の結果から，タバコ培養細胞は B 欠乏に際して酸化障害を回避・修復する代謝応答を示すものの，本来 B が果たしている機能を他の因子で代替する手段を持たないため，酸化ストレスが継続し結局はネクローシスに至ると推測した．

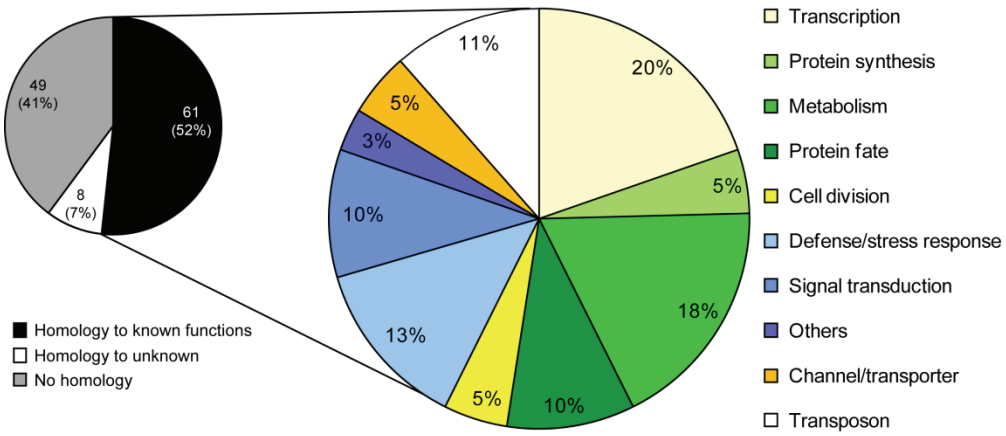

Fig. 3 B 欠乏応答性遺伝子の分類．機能が推定できた遺伝子の比率（左）とそれらの遺伝子の機能別分類（右）．

3. ホウ素欠乏感知機構の解析

–B 処理によるストレス応答性遺伝子の発現を RT-PCR で解析したところ，処理後 1 時間以内に誘導が観察された（Fig. 4a）．このことは培地からの B の消失は短時間のうちに細胞に感知されることを示唆する．これら遺伝子の発現変化は培地 Ca^{2+}の除去（Fig. 4a）あるいは Ca^{2+}チャネルブロッカーである La^{3+}の添加（Fig. 4b）で抑制されたことから，Ca^{2+}チャネルからの Ca^{2+}流入が B 欠乏応答を引き起こすと推測した．

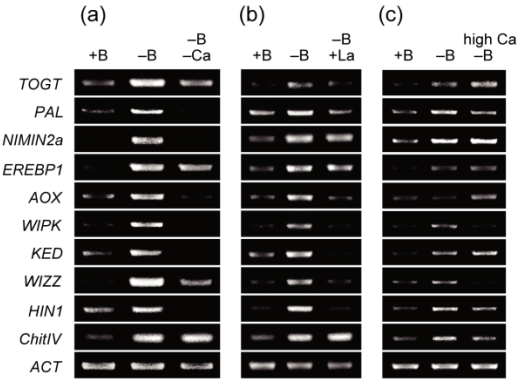

Fig. 4 –B 処理後 1 時間におけるストレス応答性遺伝子の発現変化．(a) 遺伝子の発現誘導に対する Ca^{2+}除去の影響. (b) 遺伝子の発現誘導に対する La^{3+}添加の影響．(c) 30 mM Ca^{2+}を含む培地で 1 時間前培養後に–B 処理したときの遺伝子の発現変化.

そこで Ca^{2+}と結合し Ca^{2+}濃度依存的に発光するエクオリンを発現する細胞を用い，–B 処理に伴う Ca^{2+}流入を検討した．まず細胞を 20 μM Ca^{2+}を含む–B 培地あるいは+B 培地で洗浄し，同じ培地中で 5 分間インキュベートした後に培地 Ca^{2+}濃度を 3 mM に上昇させた．–B 刺激により Ca^{2+}チャネルが開口するならば，培地 Ca^{2+}濃度を上昇させた際に–B 細胞には+B 細胞より多くの Ca^{2+}が流入し，より強い発光が観察されることが期待される．実験の結果，–B 処理細胞では+B 処理細胞の約 2 倍の Ca^{2+}流入が観察された（Fig. 5a）．発光は La^{3+}の添加で完全に抑制された（Fig. 5b）ことから，この Ca^{2+}流入はチャネルを経由したものである．また洗浄開始から Ca^{2+}添加処理までは 7 分しか要していない．つまり，培地からの B 除去は 7 分以内に Ca^{2+}チャネルを開口させ，–B 応答を引き起す．これは養分欠乏シグナルの伝達に Ca^{2+}が関与することを示した初めての例である．NADPH oxidase の阻害剤である diphenylene iodonium（DPI）が–B 細胞への Ca^{2+}流入を抑制した（Fig. 5b）ことは，この Ca^{2+}チャネルの活性化に ROS が関与することを示唆する．

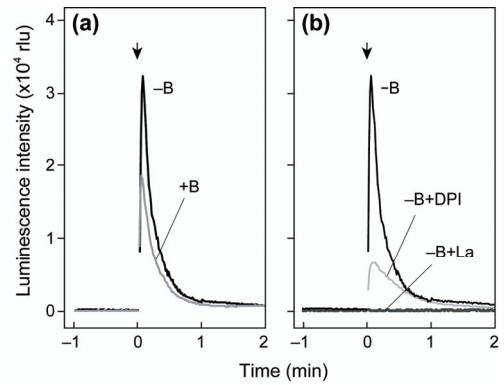

Fig. 5 –B 処理によるエクオリン発光の強度変化．矢印の時点で終濃度が 3 mM となるように Ca^{2+}を添加した．(a) +B と–B 処理での比較．(b) La^{3+}や DPI が–B 処理による発光に与える影響.

B 欠乏が Ca^{2+}チャネルを開口させるメカニズムとして， ペクチン質多糖の RG-II 領域が架橋されないことで細胞壁の物理的強度が低下し，原形質の吸水拡大による原形質膜の伸展が起こる．その結果，原形質膜上の伸展活性化 Ca^{2+}チャネルが開口すると考えた．この仮説が正しければ，細胞壁構造の強化や原形質膜の伸展抑制によって B 欠乏応答が抑制されるはずである．そこで高濃度（30 mM）Ca^{2+}を含む培地で細胞を前培養し，Ca^{2+}-ポリガラクツロン酸架橋の密度を高めて細胞壁構造を強化した後に細胞を–B 処理したところ，B 欠

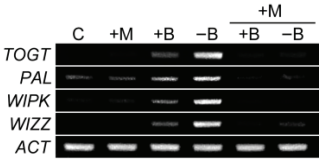

Fig. 6 高浸透圧処理による–B 遺伝子の発現抑制. C, 無処理; +M, 0.4 M マンニトール，+B, +B 処理; –B，–B 処理.

乏応答性遺伝子のうち *WIPK* と *WIZZ* の発現が強く抑制された（Fig. 4c）．また，原形質膜の伸展を抑制するために高浸透圧条件下で–B 処理を行うと *TOGT*，*PAL*，*WIPK*，*WIZZ* の発現誘導は抑制された（Fig. 6）．これらの結果は，B 欠乏による細胞壁の物理的強度の低下が Ca^{2+}チャネルの開口を引き起こすという仮説を支持する．

以上の結果から，B 欠乏応答について Fig. 7 のようなスキームを提唱する．B が欠乏すると RG-II の架橋不全が起こり，細胞壁の物理的強度を低下させる．これにより原形質膜が伸展して伸展活性化 Ca^{2+}チャネルが開口し，Ca^{2+}流入と遺伝子の発現変化を引き起こす．流入した Ca^{2+} は NADPH oxidase の活性化により ROS の生成を促進する．細胞は B 欠乏で発生する酸化ストレスに応答し抵抗反応や修復応答を誘導するが，必須元素である B の機能を代替する手段を持たないため B 欠乏状態は改善されず，断続的な Ca^{2+}流入と ROS の生成が繰り返される結果，最終的に酸化障害によるネクローシスが起こると考えられる．

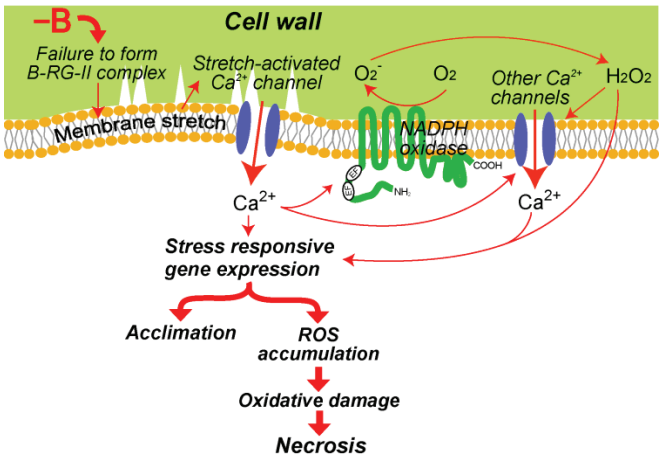

Fig. 7 B 欠乏応答のスキーム

要約

(1) ホウ素欠乏による細胞死は酸化障害を直接の原因とするネクローシスであることを明らかにした．

(2) ホウ素欠乏に伴う遺伝子発現変化のマイクロアレイ解析により，障害からの回復やストレス応答に関する遺伝子の発現が誘導されることを明らかにした．一方，ホウ素の機能を代替し得るような因子は誘導されず，タバコ培養細胞はホウ素欠乏を回避する有効な手段を持たない可能性を示した．

(3) タバコ培養細胞はホウ素欠乏をすばやく感知すること，このホウ素欠乏シグナルの伝達に Ca^{2+}が関与することを示した．またこの Ca^{2+}チャネルの開口が細胞壁構造の異常によって引き起される可能性を示した．